AN ABSTRACT OF THE THESIS OF

Owen L. Stevens for the degree of Master of Science in Nuclear Engineering and Mechanical Engineering presented on June 7, 1996. Title: Characterization of the Advanced Plant Experiment (APEX) Passive Residual Heat Removal System Heat Exchanger.

Redacted for Privacy

Abstract approved: _____

Jose N. Reyes Jr.

Redacted for Privacy

Abstract approved: _____

Lorin R. Davis

The Oregon State University (OSU) Radiation Center (RC) is the location of a one quarter scale model of the Westinghouse Electric Corporation advanced light-water nuclear reactor design called the AP-600. The full scale AP-600 is a 600 megawatt electric nuclear power plant that incorporates unique passive systems to perform the safety functions currently required of all existing nuclear power plants. Passive safety refers to a system's ability to perform its desired function using natural forces such as gravity and natural circulation. This reduces the reliance on active systems to assure plant safety.

The Advanced Plant Experiment (APEX) at the OSU RC is an electrically heated simulation of the AP-600 that includes the Nuclear Steam Supply System (NSSS) and all of the passive safety systems. The APEX facility was funded by the United States Department of Energy and the Westinghouse Electric Corporation. The facility was built to perform the long term cooling tests necessary for design certification of the AP-600. The data taken will be used to benchmark the thermal hydraulic computer codes applied in the design certification process and to better understand the phenomena involved in the full scale AP-600.

This paper presents the analysis of the Passive Residual Heat Removal System (PRHR) and in particular the PRHR's "c"-shaped heat exchanger (PRHR Hx). This paper

includes analysis and modeling of the PRHR Hx including: hydraulic flow parameters, heat rejection capability, an empirical correlation for determining pressure drop, and an examination of the flow phenomena that occurs in the tank in which the heat exchanger is installed.

Characterization of the Advanced Plant Experiment (APEX) Passive Residual Heat Removal System Heat Exchanger

by

Owen L. Stevens

A THESIS

submitted to

Oregon State University

in partial fulfillment of
the requirements for the
degree of

Master of Science

Completed June 7, 1996
Commencement June 1997

Master of Science thesis of <u>Owen L. Stevens</u> presented on <u>June 7, 1996</u>

APPROVED:

Redacted for Privacy
_____
Co-Major Professor, representing Nuclear Engineering

Redacted for Privacy
_____
Co-Major Professor, representing Mechanical Engineering

Redacted for Privacy
_____
Head of Department Nuclear Engineering

Redacted for Privacy
_____
Head of Department Mechanical Engineering

Redacted for Privacy
_____
Dean of Graduate School

I understand that my thesis will become part of the permanent collection of Oregon State University libraries. My signature below authorizes release of my thesis to any reader upon request.

Redacted for Privacy
_____
Owen L. Stevens, Author

TABLE OF CONTENTS

TABLE OF CONTENTS (Continued)

TABLE OF CONTENTS (Continued)

LIST OF FIGURES

LIST OF FIGURES (Continued)

LIST OF TABLES

NOMENCLATURE

Symbol	Definition
A,	Surface area; ft^2, m^2; eq. (4-7)
A_1,	Method One coefficient in the numerator; eq. (3-12).
A_2,	Method Two coefficient in the numerator; eq. (3-13).
A_3,	Method Two coefficient in the numerator; eq. (3-14).
A_i,	Wall inside area; ft^2, m^2; eq. (4-8).
A_{in},	The inlet flow area; ft^2, m^2; eq. (3-3).
A_{inlet},	PRHR Hx inlet area; ft/s, m/s; eq. (3-18).
A_o,	Wall outside area; ft^2, m^2; eq. (4-8).
A_{out},	The outlet flow area; ft^2, m^2; eq. (3-3).
A_{tube},	PRHR Hx tube area; ft^2, m^2; eq. (3-18).
B,	Method One exponent of the Reynold's number; eq. (3-12).
cs,	Control Surface; eq. (4-1).
cv,	Control volume; eq. (4-1).
Cp,	Constant pressure specific heat; Btu/(lbm*°F), J/(kg*K); eq. (4-6)
D_{tube},	PRHR Hx tube diameter; ft , m; eq. (3-24).
e,	Specific energy; Btu/lbm, J/kg; eq. (4-1).
f_D,	Darcy friction factor.
g,	The acceleration of gravity; ft^2/s, m^2/s; eq. (3-3).

g_c,	The conversion factor to convert from lbf to lbm; $lbm*ft/(lbf*s^2)$; eq. (3-1).
h,	Convective heat transfer coefficient; $Btu/(hr*ft^2*°F)$, $W/(m^2*K)$; eq. (4-7).
h_i,	Inside convective heat transfer coefficient; $Btu/(hr*ft^2*°F)$, $W/(m^2*K)$; eq. (4-8).
h_{in},	Inlet enthalpy; Btu/lbm, J/kg; eq. (4-4).
$h_{L_A}, h_{L_B}, h_{L_C}, \cdots$,	PRHR Hx tube row head loss, i.e. h_{L_A} is the tube row A head loss, $\Delta P/\rho$; ft lbf/lbm, $Pa/(kg*m^3)$; eq. (3-19).
h_o,	Outside convective heat transfer coefficient; $Btu/(hr*ft^2*°F)$, $W/(m^2*K)$; eq. (4-8).
h_{out},	Outlet enthalpy; Btu/lbm, J/kg; eq. (4-4).
$k_{T_A}, k_{T_B}, k_{T_C}, \cdots$,	PRHR Hx tube row hydraulic resistance coefficient, i.e. k_{T_A} is the tube row A velocity; ft/s, m/s; eq. (3-20).
k_{tube},	PRHR Hx tube hydraulic resistance coefficient; eq. (3-27).
k_w,	Wall thermal conductivity; $Btu/(hr*ft*°F)$, $W/(m*K)$; eq. (4-8).
$K_{additional}$,	Added hydraulic resistance coefficient; eq. (3-29).
$K_{form\ losses}$,	Portion of the coefficient of hydraulic resistance due to form losses; eq. (3-10).
$K_{frictional\ losses}$,	Portion of the coefficient of hydraulic resistance due to frictional losses; eq. (3-10).
K_{total},	Total coefficient of hydraulic resistance; eq. (3-1).

$K_{total\ losses}$,	Total coefficient of hydraulic resistance, the sum of form and frictional losses; eq. (3-10).
L,	Tube length; ft, m; eq. (4-8).
L/D,	Tube length over diameter ratio, also known as the pipe ratio; eq. (3-17).
m,	Mass; lbm, kg; eq. (3-3).
$\dot{m}$,	Mass flow rate; lbm/s, kg/s; eq. (3-3).
p_{in},	Inlet pressure; atm, Pa; eq. (3-3).
p_{out},	Outlet pressure; atm, Pa; eq. (3-3).
Q,	Heat transfer; BTU, J; eq. (4-7)
r_i,	Wall inside radius; ft, m; eq. (4-8).
r_o,	Wall outside radius; ft, m; eq. (4-8).
R^2,	Coefficient of determination short-hand notation; eq. (3-16).
Re,	Reynold's number, defined as $\rho v D / \mu$; eq. (3-12).
Re_{tube},	PRHR Hx tube Reynold's number; eq. (3-24).
R_{fi},	Inside fouling resistance; hr*ft^2*°F/Btu, m^2*K/W; eq. (4-8).
R_{fo},	Outside fouling resistance; hr*ft^2*°F/Btu, m^2*K/W; eq. (4-8).
t,	Time; hr, s; eq. (4-1).
t_1,	Surrounding fluid inlet temperature; °F, K; eq. (4-10).
t_2,	Surrounding fluid outlet temperature; °F, K; eq. (4-10).

T_1,	Hx inlet fluid temperature; °F, K; eq. (4-10).
T_2,	Hx outlet fluid temperature; °F, K; eq. (4-10).
u_{in},	Inlet internal energy; Btu/lbm, J/kg; eq. (4-3).
u_{out},	Outlet internal energy; Btu/lbm, J/kg; eq. (4-3).
U,	Overall heat transfer coefficient; Btu/(hr*ft^2*°F), W/(m^2*K); eq. (4-8).
v,	The fluid velocity; ft/s, m/s; eq. (3-1).
v_A, v_B, v_C,...,	PRHR Hx tube row velocity, i.e. v_A is the tube row A velocity; ft/s, m/s; eq. (3-18).
v_{inlet},	PRHR Hx inlet velocity; ft/s, m/s; eq. (3-18).
v_{tube},	PRHR Hx tube velocity; ft/s, m/s; eq. (3-25).
v'_{tube},	PRHR Hx tube provisional velocity; eq. (3-27).
V,	Volume; ft^3, m^3; eq. (4-1).
W_μ,	Frictional work; Btu, J; eq. (4-1).
W_S,	Shaft work; Btu, J; eq. (4-1).
X,	Velocity weighting factor; eq. (3-23).
z_{in},	Inlet elevation; ft, m; eq. (3-3).
z_{out},	Outlet elevation; ft, m; eq. (3-3).
μ,	Viscosity of water; lbm/ft s, Pa s; eq. (3-25).
ρ,	The density of water; lbm/ft^3, kg/m^3; eq. (3-1).
ρ_{in},	The inlet density of water; lbm/ft^3, kg/m^3; eq. (4-3).
ρ_{out},	The outlet density of water; lbm/ft^3, kg/m^3; eq. (4-3).

$\Delta p_{\text{form losses}}$,   Pressure drop due to form losses; atm, Pa; eq. (3-9).

$\Delta p_{\text{frictional losses}}$,   Pressure drop due to frictional losses; atm, Pa; eq. (3-9).

Δp_{loss},   Inlet to outlet pressure drop; atm, Pa; eq. (3-3).

$\Delta p_{\text{total looses}}$,   Total pressure drop due to losses; atm, Pa; eq. (3-9).

ΔP,   Pressure drop or delta pressure; atm, Pa; eq. (3-1).

ΔT,   Temperature difference between object and medium; °F, K; eq. (4-7).

ΔT_{LMTD},   Log mean temperature difference; °F, K; eq. (4-9).

Characterization of the Advanced Plant Experiment (APEX) Passive Residual Heat Removal System Heat Exchanger

1.   Introduction

In many complex systems it is possible to analyze individual components in detail and then combine the results for a global analysis of the system. The problem presented in this document is the mathematical modeling of the Passive Residual Heat Removal System (PRHR) Heat Exchanger (Hx) of the Westinghouse advanced light-water nuclear reactor design called AP-600. The PRHR Hx is the key component of the PRHR system which has been physically simulated on a scaled basis in the Oregon State University (OSU) Advanced Plant Experiment (APEX) test facility. The analysis includes a fluid flow bench test, hydraulic modeling of the PRHR Hx, model comparisons to APEX test data, an examination of the PRHR Hx heat rejection capability, and a study of the flow phenomena in the tank in which the PRHR Hx is placed. The objectives of the analyses are:

- Perform a bench flow test of the PRHR Hx to obtain a set of pressure drop measurements across the heat exchanger at various fluid flow rates.

- Develop a model of the hydraulic resistance of the heat exchanger using the bench test data.

- Create a PRHR thermal hydraulic database from APEX Integral System test data.

- Study the heat rejection capability of the PRHR Hx in various operating conditions, including natural circulation and forced flow.

- Compare heat rejection ability to IRWST fluid temperature stratification.

- Study the effects of boiling on PRHR Hx heat rejection and other phenomena that develop in the IRWST.

Chapter two is a description of the APEX test facility, and the function of the PRHR. Chapter three contains the hydraulic characterization of the PRHR Hx. Chapter four is the thermal characterization of the PRHR Hx. The fifth chapter examines the PRHR Hx and IRWST in a station blackout simulation. Finally, chapter six presents the results of the analyses and gives recommendations for further research.

2. Description of the APEX PRHR System

The OSU Radiation Center (the location of the Oregon State University Department of Nuclear Engineering) houses a one quarter scale model of the Westinghouse Electric Corporation advanced light-water nuclear reactor design called AP-600. The AP-600 reactor design incorporates many passive safety features for reactor core cooling. In this case, passive means that the systems are capable of core cooling using only the phenomena of gravity driven flow and natural convection of heated fluids. The model of the AP-600 (APEX) was built to perform the testing necessary for design certification.

APEX operates at 2.76 MPa (400 Psia) and has been formally scaled[1] to simulate the important thermal hydraulic behavior of the AP-600. APEX is electrically heated and simulates the nuclear steam supply system (NSSS) and all of the AP-600 safety systems. The systems modeled include the primary system, passive safety systems, the non-safety grade chemical and volume control system, and the residual heat removal system (PRHR).

APEX is operated in accordance with ASME NQA-1[2] because it will be used for AP-600 design certification. The specific requirements for instrument calibration and records have been met as established in Appendix B of Title 10 Part 50 of the Code of Federal Regulations[3]. Quality assurance (QA) procedures have been implemented in accordance with a Project Quality Plan[4] and facility audits have been performed by the US Nuclear Regulatory Commission, Westinghouse QA, and the US Department of Energy. The general plant layout is shown in Figures 2.1 and 2.2.

2.1   APEX Primary System

The APEX primary system consists of the following components:

- The Reactor Pressure Vessel models the upper and lower reactor internals, the core barrel, the downcomer, and the core. Connections for hot and cold legs and direct vessel injection (DVI) lines are provided. The reactor vessel houses 48 electric heater rods which give a maximum core power of 600 kW.

- The Reactor Coolant Loop Piping models two primary loops, each consisting of one hot leg and two cold legs. Break spool pieces are installed on the hot and cold legs, the DVI line, and the core makeup tank (CMT) pressure balance line to simulate pipe breaks. The discharge from these breaks vents to the break and automatic depressurization system measurement system (BAMS). The BAMS is used to measure the break and ADS vapor and liquid volumetric flow rates.

- Two Steam Generators (SGs), one on each loop, have tube and shell dimensions scaled to model the Westinghouse Delta-75 steam generator design.

- Four Reactor Coolant Pumps (RCPs) are used - two attached to the lower channel head of each SG.

- A Pressurizer that has internal heaters capable of controlling pressure and minimizing pressure spikes in the reactor cooling system.
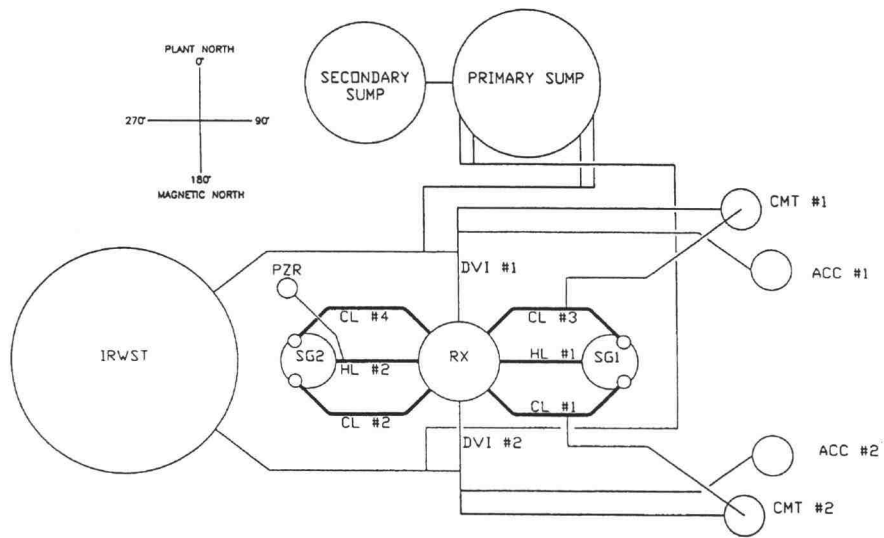
Figure 2.1   APEX Test Facility Line Diagram
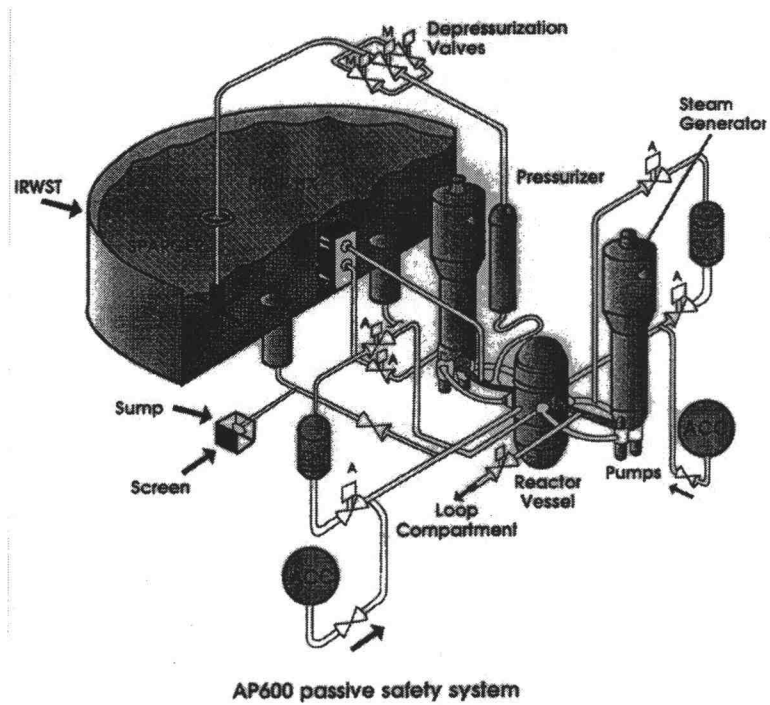
Figure 2.2   APEX Test Facility Layout Diagram

2.2   APEX Passive Safety System

The APEX test facility includes the following passive safety systems:

- Two Core Makeup Tanks (CMTs) each having a pressure balance line that connects the CMT head to the cold leg. Each CMT also has an injection line that permits draining into one of the two DVI lines. Check valves and isolation valves have been included.

- An In-containment Refueling Water Storage Tank (IRWST) that has two injection lines that connect to the DVI. The IRWST can be pressurized to 550 kPa to simulate containment back pressure.

- An Automatic Depressurization System (ADS) is included that can vent the pressurizer by means of three valves. These valves vent into a sparger in the IRWST. The fourth ADS valve vents the hot legs to the primary sump.

- Two Accumulators pressurized with nitrogen provide safety injection during depressurization events. Each accumulator connects to a DVI line.

- A Passive Residual Heat Removal (PRHR) system that is detailed below.

2.3   APEX PRHR System

The PRHR system is designed to remove residual heat from the reactor core before the main safety systems have injected their water and the reactor vessel has been de-pressurized to atmospheric pressure. Figure 2.3 is a schematic of the PRHR system. The PRHR system provides cooling using the very large In-containment Refueling Water Storage Tank (IRWST) as its ultimate heat sink. The system is cooled by means of gravity driven flow and natural convection of heated fluids through the PRHR Hx. The PRHR Hx resides inside the IRWST. The inlet piping of the PRHR Hx is connected to the fourth stage automatic depressurization system (ADS) line which is attached to one of the hot legs. The outlet piping of the PRHR Hx is connected to the cold side plenum of one of the steam generators.

The heat source for the PRHR system is the primary side of APEX. The primary side is at high pressure to prevent boiling in the core. The primary side includes the heat producing core, the steam generators, the pressurizer and all the connecting piping. The primary system provides the heat that will be removed by the PRHR and also the pathway to the core.

The heat sink for the PRHR is the IRWST. The volume of water contained in the IRWST in the AP-600 is such that if all of it is injected into the primary system, the reactor vessel will be below the water level in containment (the break leaks into containment). In APEX, the IRWST contains approximately 3000 gallons of water. The IRWST liquid is at containment pressure and initially at containment temperature. Injection from the IRWST can be used to cool the primary system but this occurs after PRHR operation so it will not be discussed in this paper.
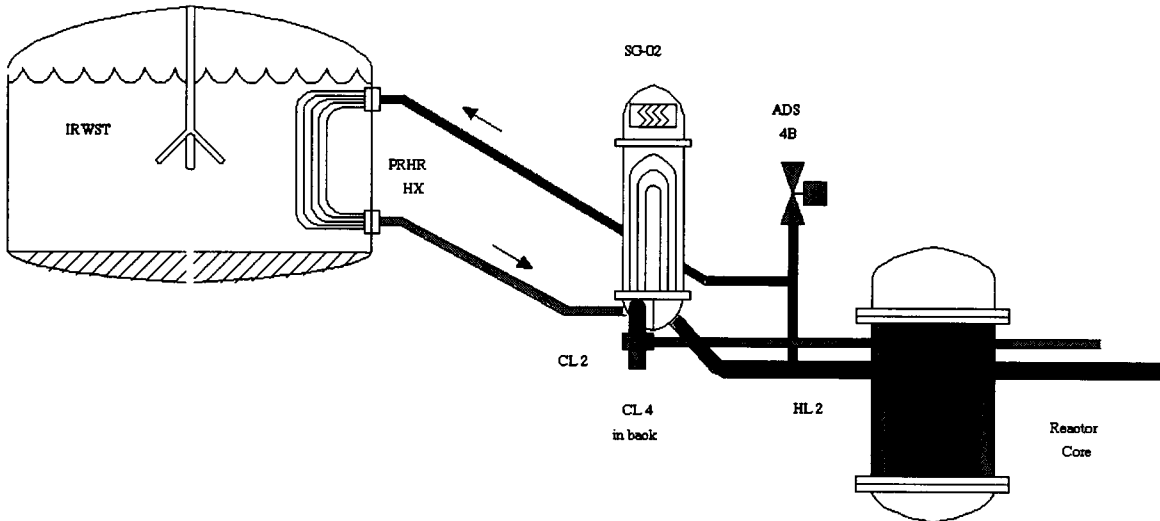
Figure 2.3   APEX PRHR System Schematic

The APEX PRHR Hx is shown in Figure 2.4. It is a "C" type shell and tube heat exchanger consisting of 88 stainless tubes arranged in a square array. Each tube has an inside diameter of 0.25 inches. The inlet and outlet lines of the PRHR Hx are connected to plena which are attached to the inside of the IRWST, see Figure 2.5. The tube side of the PRHR Hx is at full system pressure and temperature.

In the event of a simulated pipe break the APEX reactor shuts-down switching the electrical heaters from simulated full-power operation to a simulated decay-heat mode and an "S" signal is generated. The "S" signal triggers the PRHR Hx isolation valves to open and allows the PRHR Hx to remove heat. The PRHR system takes water from the hot leg of the reactor, runs it through the PRHR Hx and then injects into the steam generator cold side plenum. In this re-circulation mode the reactor can be cooled if the IRWST level is sufficient to cover all or part of the PRHR Hx.

The advantage of such a system is obvious. Because it is a buoyancy driven process, driven by the temperature difference between the core and the IRWST liquid, no active pumps are needed to provide cooling to the core. However, being a buoyancy driven process also introduces some modeling questions, because the PRHR Hx flow rate

and heat rejection capability are coupled to the core power, which is decaying with time, and to the IRWST liquid temperature which is increasing with time.
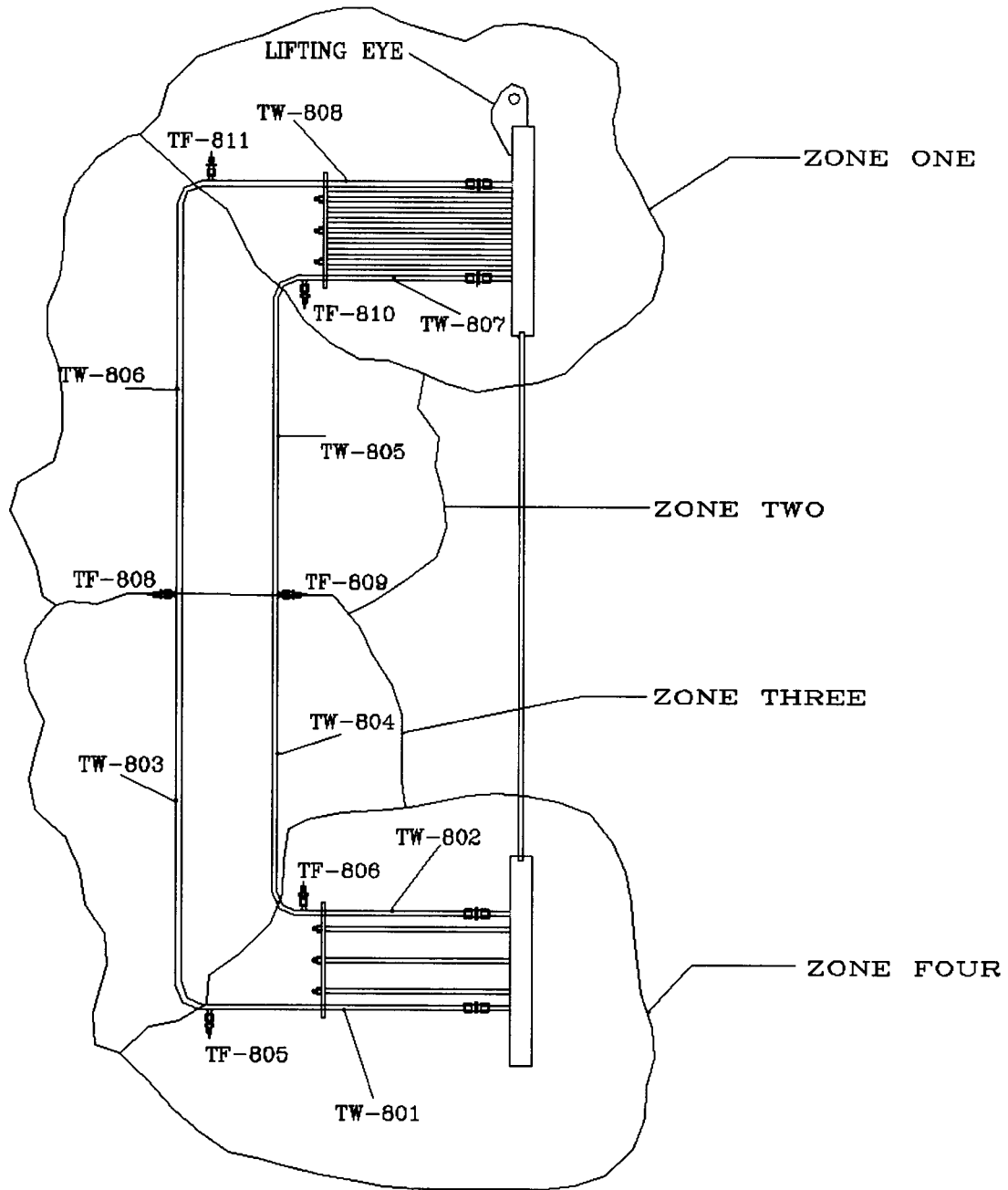
Figure 2.4   APEX PRHR Hx Zones

2.4   APEX PRHR Instrumentation

The PRHR system is instrumented with both thermocouples and flow meters. The thermocouples from the IRWST thermocouple rake are shown in Figure 2.5. The PRHR Hx thermocouples are shown in Figure 2.4. A description of each type of instrument is given below.

- Fluid thermocouples (TF) are used to measure the fluid temperature at the inlet and outlet of the PRHR loop, and to measure fluid temperature at various locations within a single outer tube and a single inner tube of the PRHR Hx.

- Wall thermocouples (TW) are attached to the tube wall surface at various locations to measure tube wall temperatures on the short (inner) and long (outer) tube of the PRHR Hx.

- Magnetic flow meters are used to measure volumetric flow in the inlet and outlet lines of the PRHR loop.
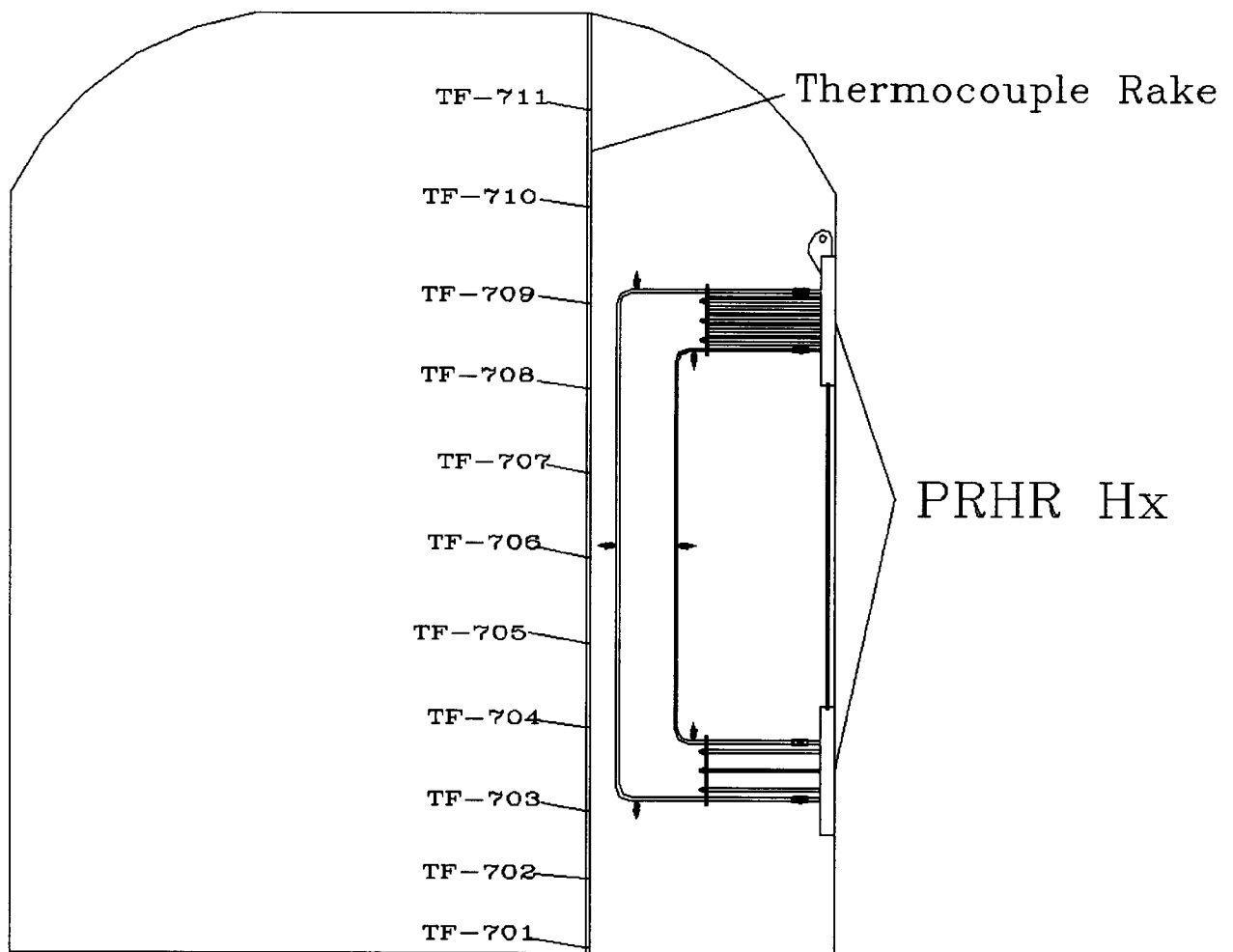
Figure 2.5   APEX PRHR Hx in IRWST

2.5   Data Acquisition and Control

The APEX data acquisition and control system (DAS) is the heart of the APEX
facility. The DAS includes all of the equipment required to collect, process, and record
the voltage and current signals from the 750 instruments installed. The DAS is a FLUKE
HELIOS system linked to three DEC 486 PC computers. The software used to process
the incoming data is made by Labveiw, and it has been validated and thoroughly tested.
The DAS is able to collect and store on compact disc all of the data from a test. Included

in the DAS system is a on-line graphical display that allows for process monitoring in conjunction with the APEX control panel.

The APEX control panel is capable of modeling all of the relevant instruments that are represented in the AP-600 model. All of the operator actions during a test are recorded by a WONDERWARE software package that was originally developed for NASA's space shuttle program. WONDERWARE has also been tested and validated.

3. Hydraulic Characterization of the PRHR Hx

An extensive bench flow test was the first step in the characterization of the PRHR Hx. The bench test was performed with a test rig specifically built for this purpose prior to the installation of the heat exchanger. The first step was to collect pressure drop data (across the PRHR Hx) for a large range of Reynold's numbers. The data collection process is discussed in following sections.

The mapping convention shown in Figure 3.1 was adopted for the PRHR Hx tubes. The mapping convention was set so that all tubes of like tube length are grouped. The numbering system is alphanumeric: each tube being assigned a row letter (A-J) and a column number. The columns are numbered from the first tube in each row even though the tube rows have different numbers of tubes (up to ten).

The data collected consisted of sets of frequency and pressure drop at different flow rates. The frequency was first converted to velocity using the flow meter manufacturer's frequency to velocity conversion factors. Next, using the fluid physical properties and the PRHR Hx tube geometry, the flow data was expressed in terms of the Reynold's number. The pressure drop across the PRHR Hx comes from a differential pressure cell which was attached by means of special fittings across each individual PRHR Hx tube. The pressure drop was measured directly by the delta pressure cell. The measured values expressed in inches of water or psig.

Once collected the data was plotted as pressure drop versus velocity squared. The slope of the pressure drop versus velocity squared should be a linear function as would be expected from the nature of hydraulic flow resistance's. As a further test the data was plotted as the total hydraulic flow resistance coefficient (K_{total}) versus Reynold's number. A plot of K_{total} versus Reynold's number is an effective test, of the fact that the hydraulic flow resistance coefficient should be a decreasing function.
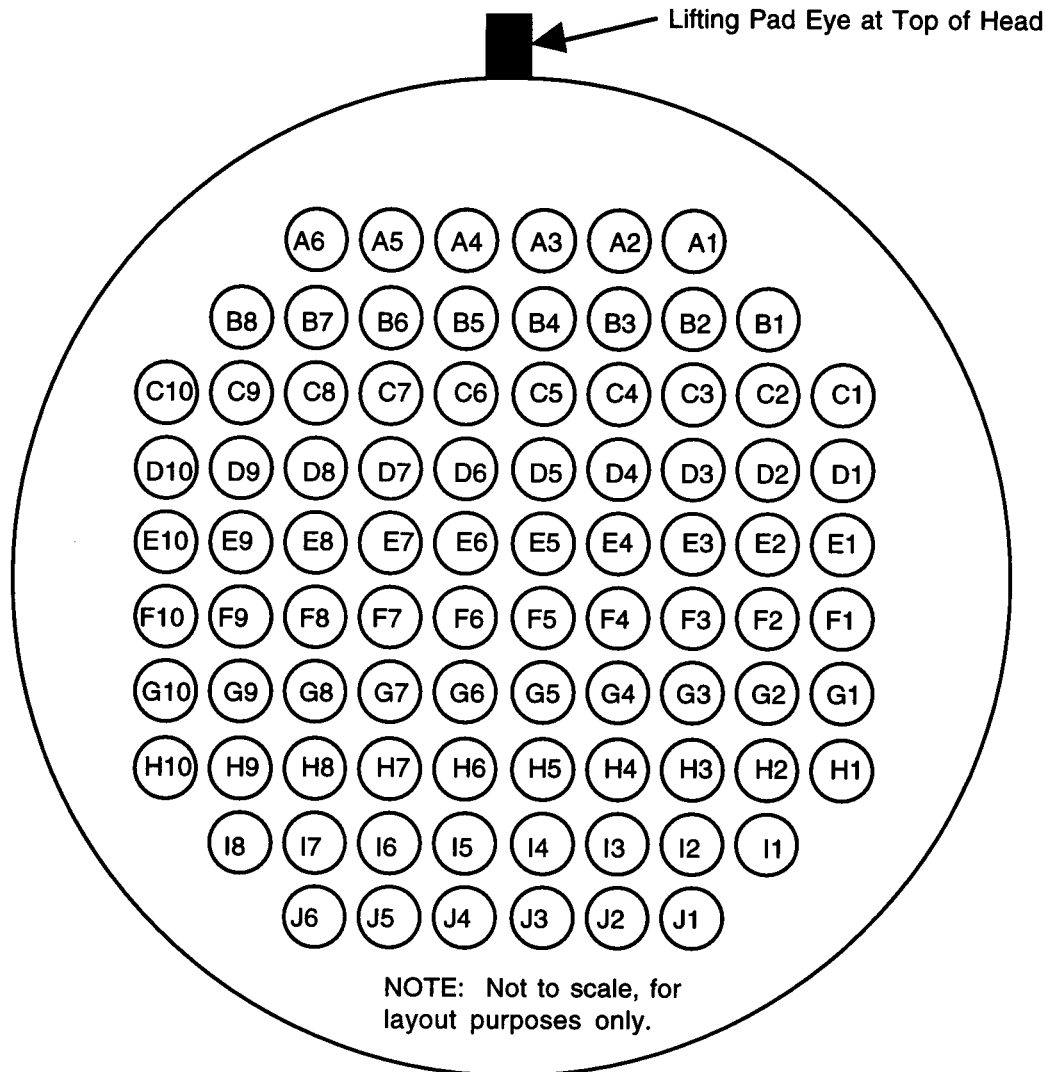
Figure 3.1 PRHR Hx Bench Flow Test Tube Map

3.1   Test Rig Description

The PRHR Hx was attached to a stand which maintained the inlet and outlet faces in a horizontal orientation. The inlet and outlet faces were maintained at the same elevation to eliminate gravity head and any gravity induced flow effects as seen in Figure

3.2. At each tube end the special fitting shown in Figure 3.3 was attached which allowed for flow in/out, and a pressure tap to be attached at the inlet and outlet PRHR Hx faces.

Flow velocity was measured in two regions, a high flow region and a low flow region. In the high flow region, a larger flow meter was used with an internal "paddle wheel" style mechanism. The delta pressure sensor for the high flow range was calibrated to read in pounds force per inch squared gauge (psig.) In the low flow region, a small flow meter was used with an internal "turbine" style mechanism. The delta pressure sensor for the low flow range was calibrated to read in inches of water (in-H_2O.) All of the pressure drop data was converted to Pascal's and all of the flow data was converted to meters per second.

The general layout of the test rig is a one-way flow path. The fluid enters a set of valves passes through the inlet fitting into the PRHR Hx tube, and then exits the outlet fitting to a drain system. The fluid used was standard Corvallis, Oregon city water at an approximate temperature of 55 ° F.
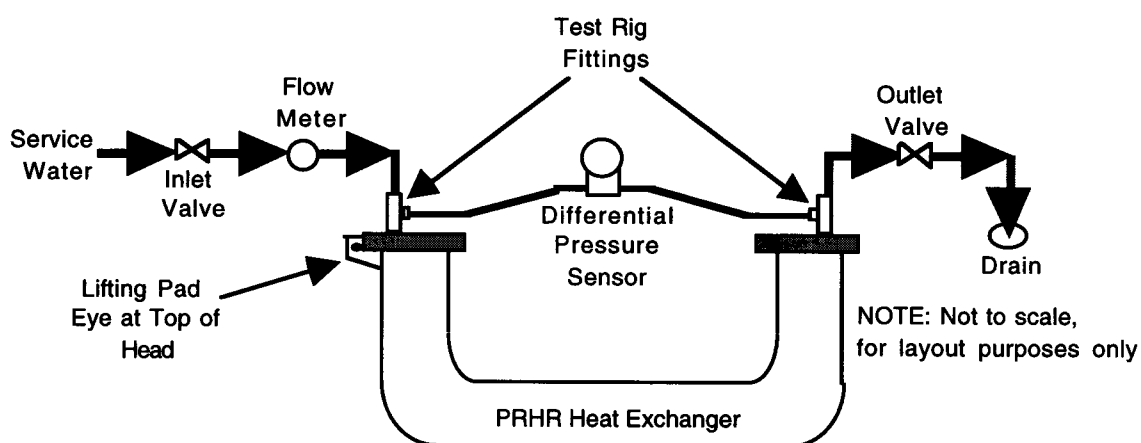
Figure 3.2   PRHR Hx Bench Flow Test Layout

3/4 inch OD (9/16 inch ID)
Tygon Tubing Clamped to
3/4 inch OD SS Tubing

1/4 inch OD (1/8 inch ID)
Tygon Tubing

SWAGELOK™ 3/4
inch SS "Tee" with
3/4 to 1/4 inch
reducer in branch
(Model # SS-12-0-0
1210-3TTF)

Stacked Rubber Washers
Over 3/4 inch OD SS
Tubing
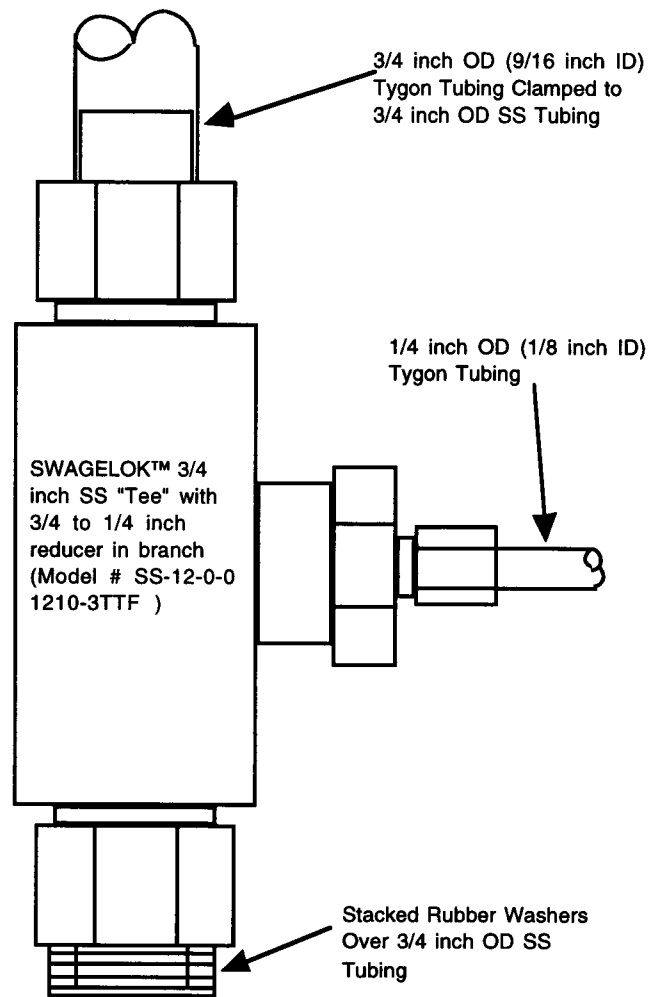
Figure 3.3 PRHR Hx Bench Flow Test, Test Rig Fitting

3.2   Procedure for Flow Test Data Collection

The general procedure was to attach the fittings to the inlet and outlet ends of a PRHR Hx tube and flow water through the tubes. The water first went through a set of valves for flow regulation and then a flow meter to obtain the meter frequency corresponding to the flow velocity. The pressure drop was measured by means of a delta pressure cell attached to the pressure taps. First, hand held instrument interfaces were

used to acquire the pressure drop in engineering units from the delta pressure cell. A fluid velocity was set using the flow meter and throttle valves. The pressure drop data was then recorded. The flow rate was allowed to stabilize to steady state flow at each velocity point. The collection procedure was performed at seven incremental velocities in each flow range. A total of fourteen data points per tube were collected for each of the 88 PRHR Hx tubes. The fluid velocity ranges were:

Low Flow Range: ~0-5 ft/s (~0-1.5 m/s), Delta Pressure: ~0-50 in of H2O (~0-12 kPa)

High Flow Range: ~ 5-25 ft/s (~1.5-7.6 m/s), Delta Pressure: ~8-40 psig (~55-275 kPa)

The resulting data set consists of 1232 data points over a flow range from almost zero to twenty five feet per second (7.6 m/s) which in turn covers a pressure drop ranging from almost zero to forty pounds per square inch gauge.

3.3   Results of Flow Test

The first task was to plot the pressure drop versus velocity squared for each of the eighty-eight PRHR Hx tubes. To reduce the number of plots, and to get the general tube row trend, the data for all tubes in each row are plotted together. In this form, the data should have a linear relationship. This is supported in Figure 3.4. All of the eighty-eight PRHR Hx tubes were plotted and all show a linear shape (see Figures 3.4 through 3.13.)
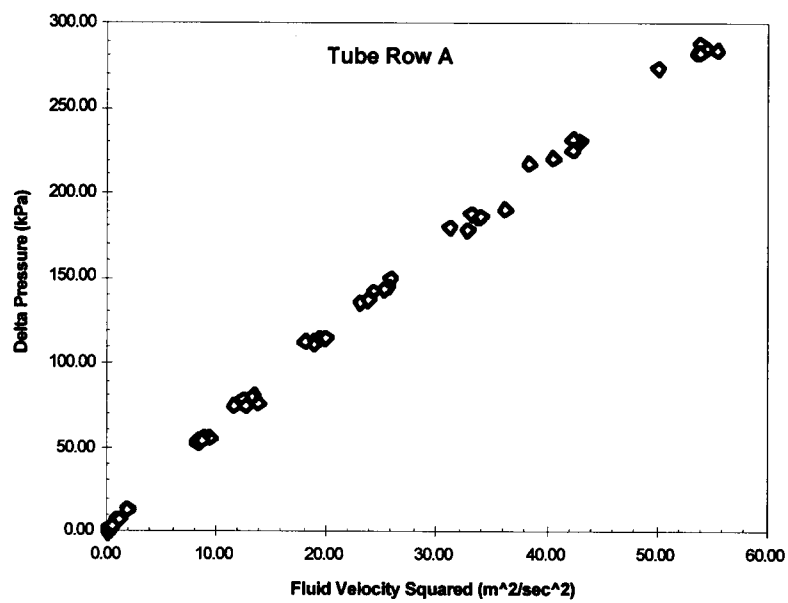
Figure 3.4   Delta Pressure vs. Fluid Velocity Squared for Tube Row A
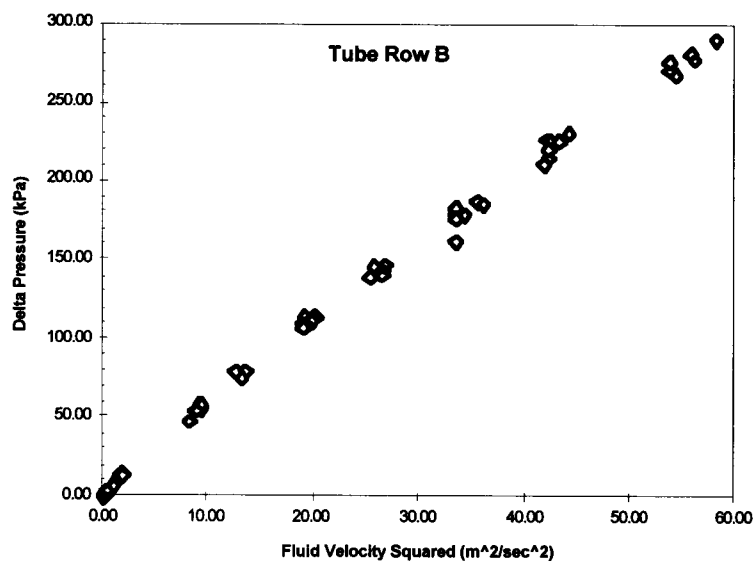
Figure 3.5   Delta Pressure vs. Fluid Velocity Squared for Tube Row B
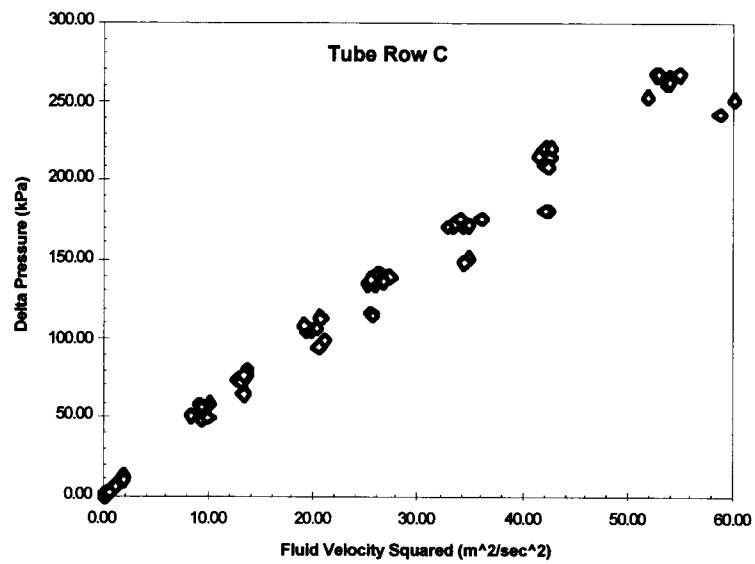
Figure 3.6   Delta Pressure vs. Fluid Velocity Squared for Tube Row C
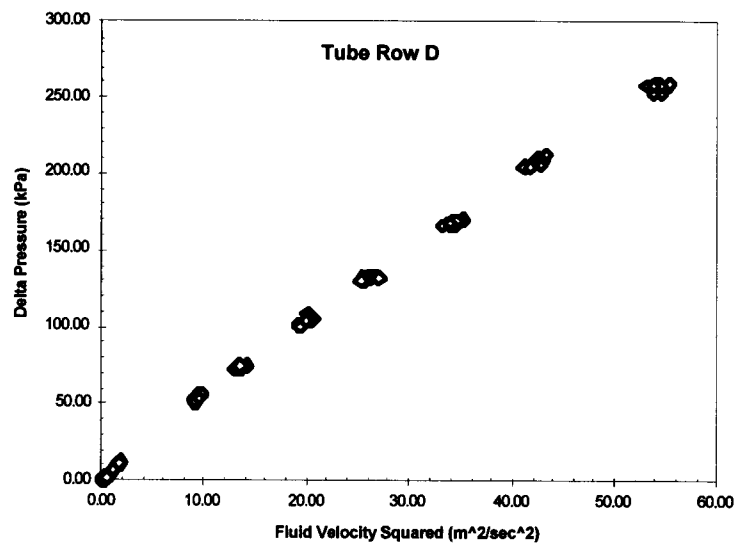
Figure 3.7   Delta Pressure vs. Fluid Velocity Squared for Tube Row D
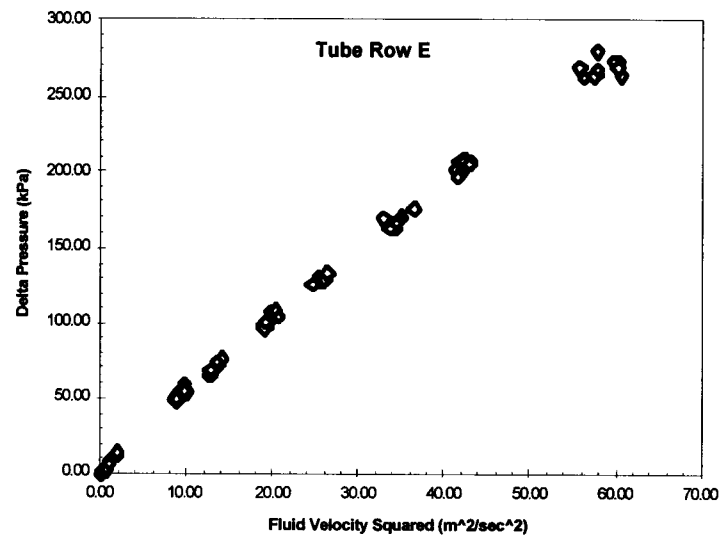
Figure 3.8   Delta Pressure vs. Fluid Velocity Squared for Tube Row E
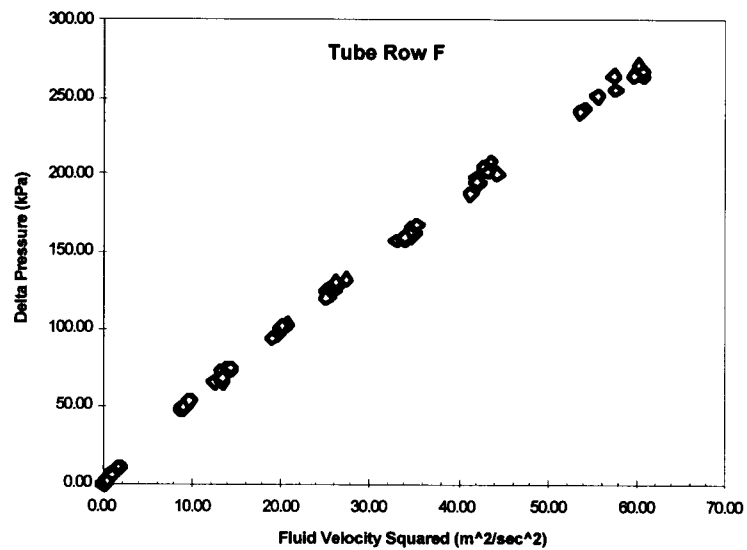
Figure 3.9   Delta Pressure vs. Fluid Velocity Squared for Tube Row F
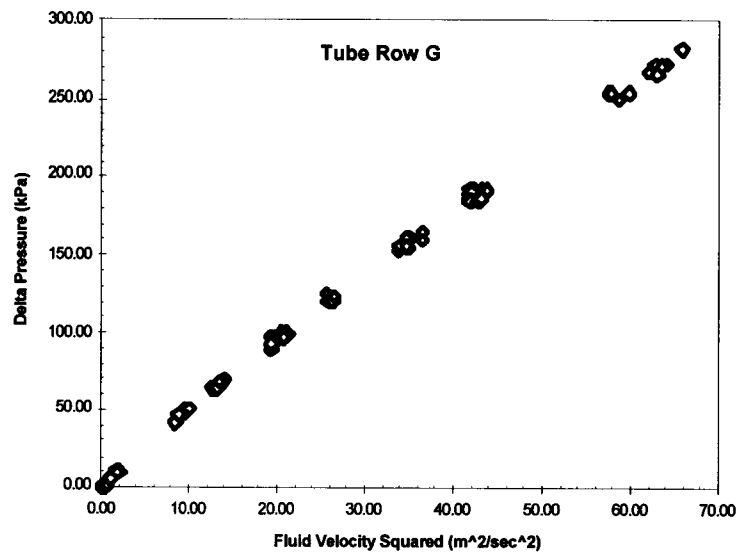
Figure 3.10   Delta Pressure vs. Fluid Velocity Squared for Tube Row G
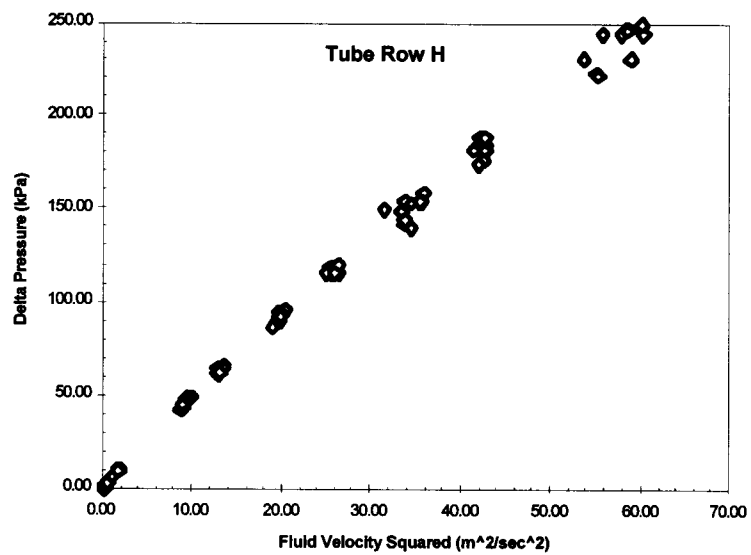
Figure 3.11   Delta Pressure vs. Fluid Velocity Squared for Tube Row H
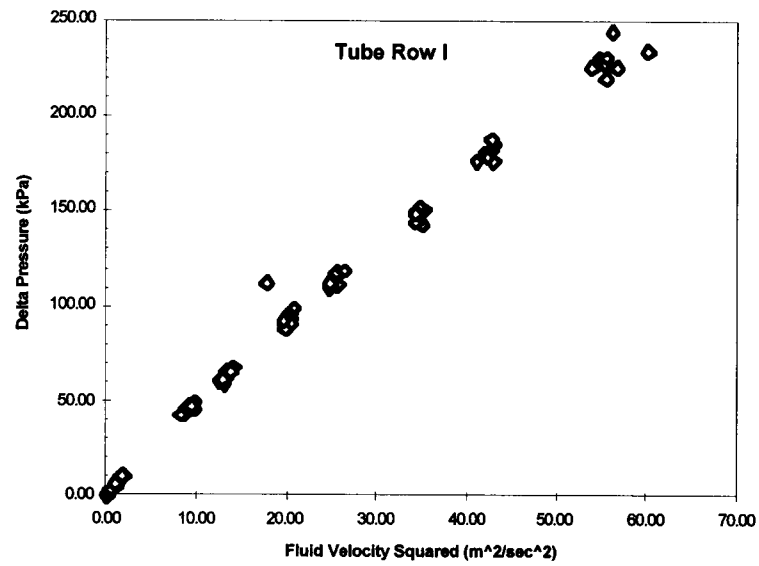
Figure 3.12   Delta Pressure vs. Fluid Velocity Squared for Tube Row I
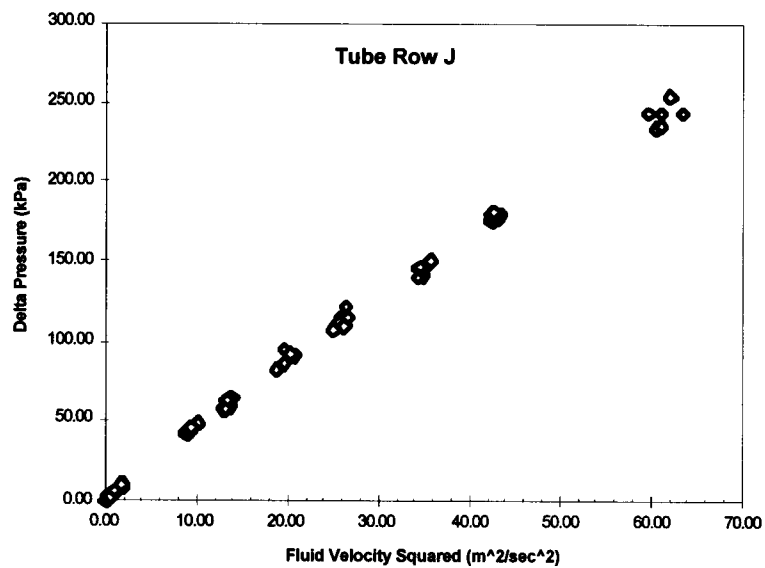
Figure 3.13 Delta Pressure vs. Fluid Velocity Squared for Tube Row J

The second task was to convert the velocity data to Reynolds numbers and then plot them versus the total head loss coefficient (K_{total}), this is shown in Figure 3.14. As before, to reduce the number of plots and to get the general tube row trend the data for all tubes in each row are plotted together (see Figures 3.14 through 3.23.) In addition, a plot of all of the data for all rows was made to show the overall trends for the heat exchanger, this is shown in Figure 3.24.

Figure 3.14 K_{total} vs. Reynold's Number for Row A
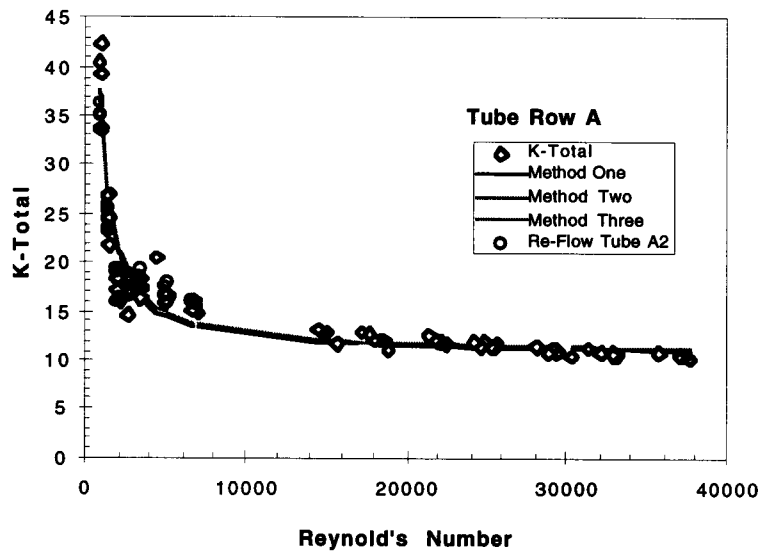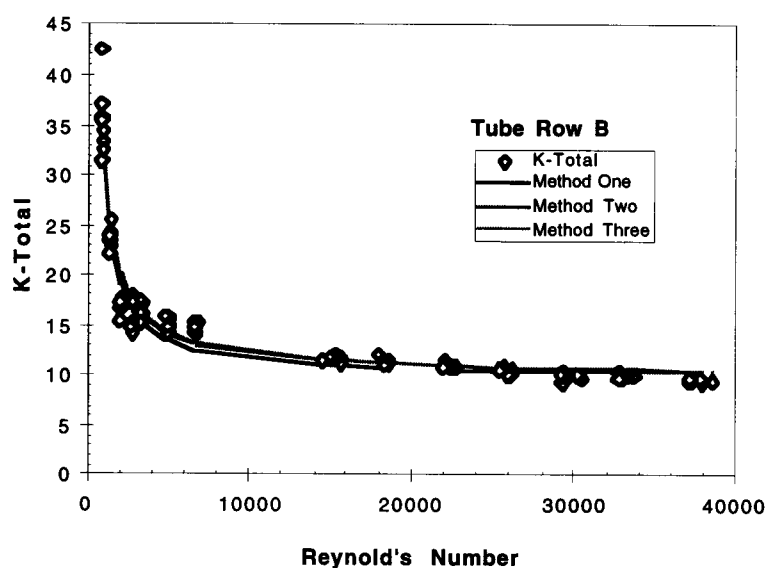
Figure 3.15 K$_{total}$ vs. Reynold's Number for Row B
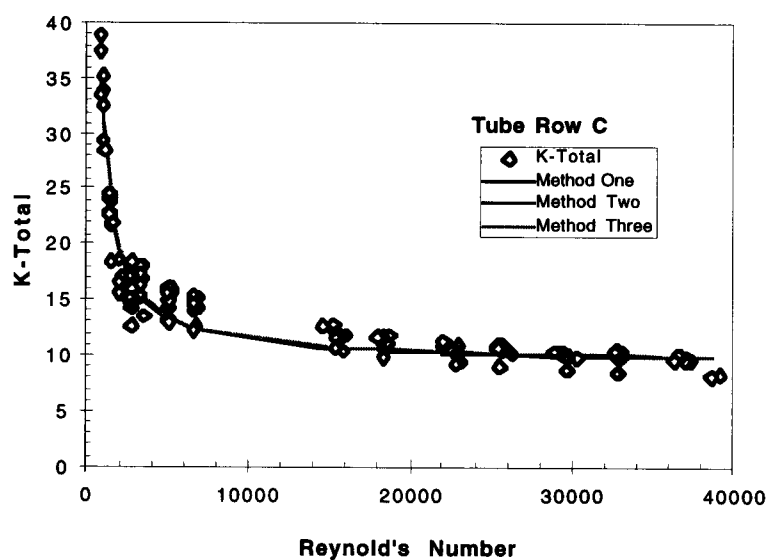
Figure 3.16 K$_{total}$ vs. Reynold's Number for Row C
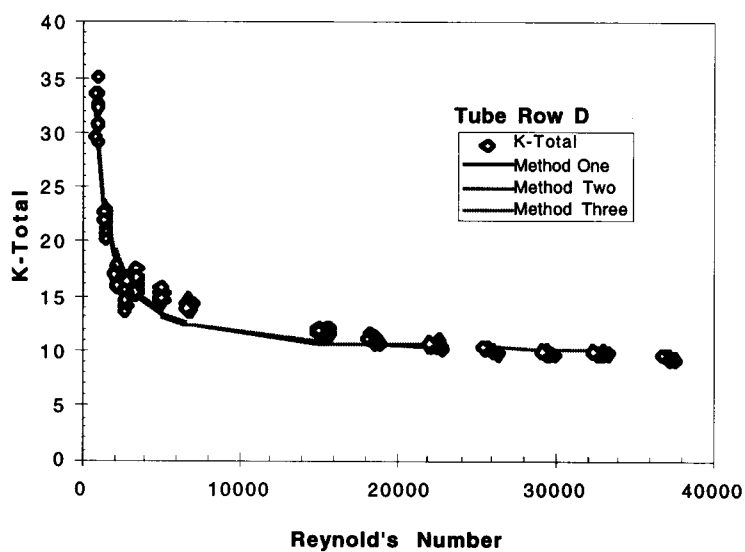
Figure 3.17 K_{total} vs. Reynold's Number for Row D
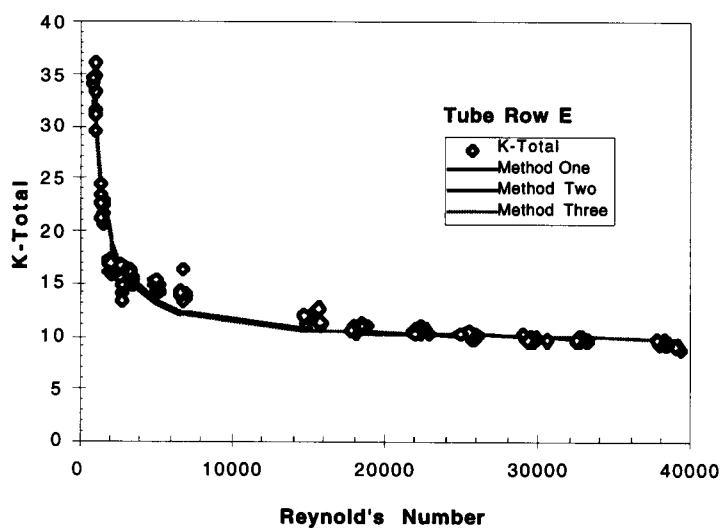
Figure 3.18 K_{total} vs. Reynold's Number for Row E
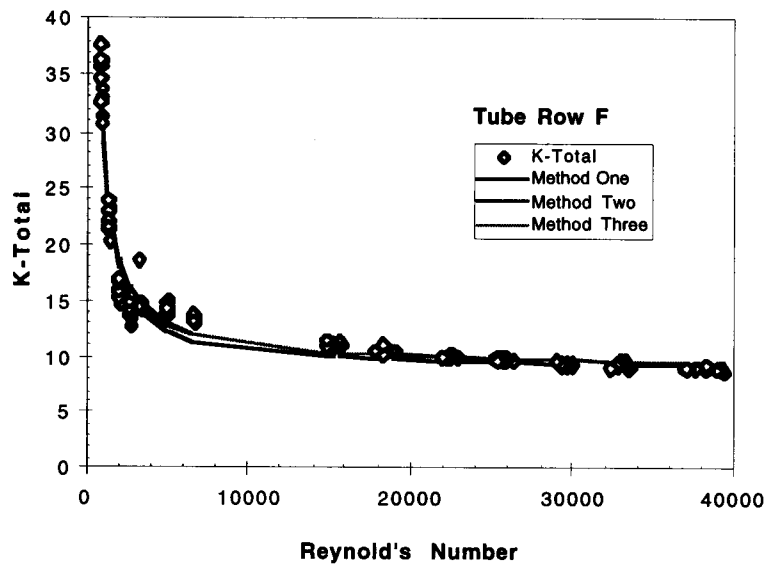
Figure 3.19   K$_{total}$ vs. Reynold's Number for Row F
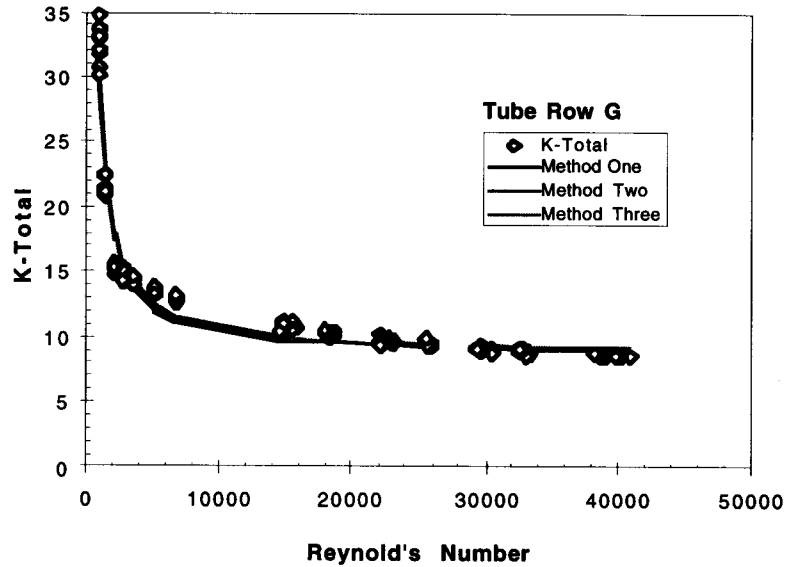
Figure 3.20   K$_{total}$ vs. Reynold's Number for Row G
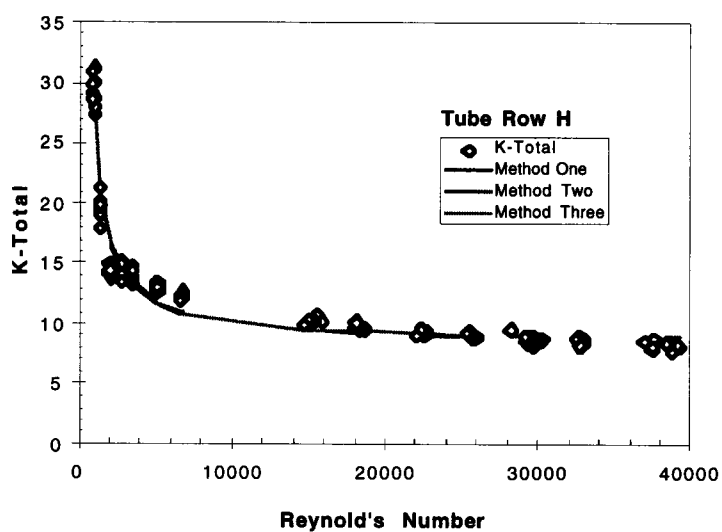
Figure 3.21   K$_{total}$ vs. Reynold's Number for Row H
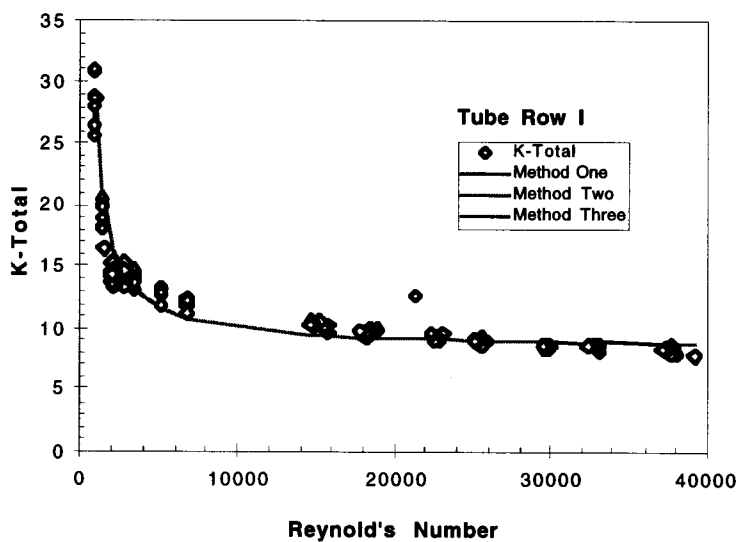
Figure 3.22   K$_{total}$ vs. Reynold's Number for Row I
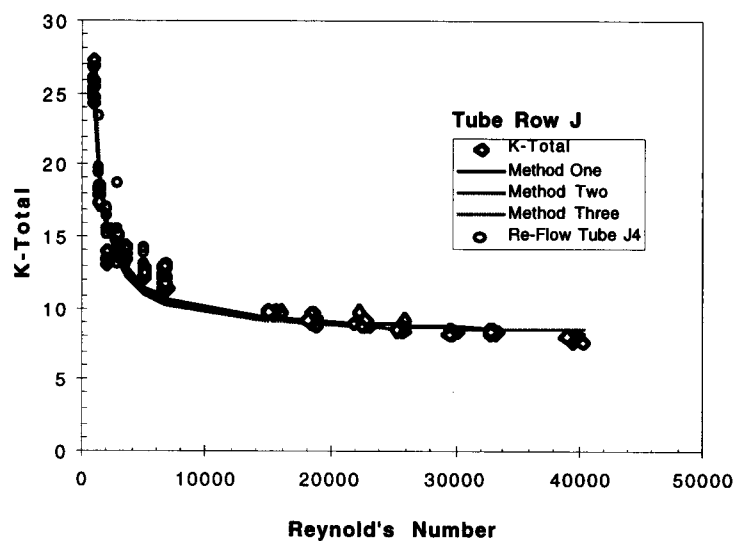
Figure 3.23 K$_{total}$ vs. Reynold's Number for Row J
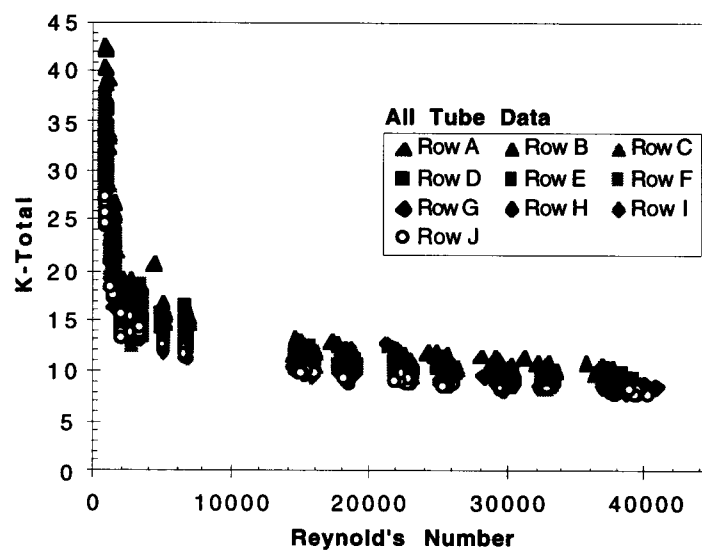
Figure 3.24 K$_{total}$ vs. Reynold's Number for All Tube Data

K_{total} comes from the definition of head loss, and head loss can be converted to pressure drop, or delta pressure. The definition of the instantaneous pressure drop[5] (delta pressure) is:

$$\Delta P \equiv \frac{K_{total}\rho v^2}{2g_c}$$

(3-1)

Solved for K_{total}, we obtain:

$$K_{total} \equiv \frac{\Delta P 2g_c}{\rho v^2}$$

(3-2)

where:

ΔP = Pressure Drop (lbf/ft^2)

ρ = Density of water (lbm/ft^3)

v = Velocity of Water in PRHR Hx Tube (ft/s)

g_c = lbf to lbm conversion factor ($lbm\ ft/lbf\ s^2$)

Looking at the plot of K_{total} versus Reynold's number for an entire row of tube data as in Figure 3.14, one can see that the data does have a generally decreasing shape much like that of one over some variable x (1/x). In general it is accepted that K_{total} will decrease (possibly exponentially) as some function of Reynold's number. The data acquired in this test is consistent with this trend. A transition is visible in the data at the approximate transition area from laminar to turbulent flow (Reynold's numbers from 2000-3000.) Closer inspection of the plot of K_{total} versus Re, reveals that a final value of eleven for K_{total} is approached at large Reynold's numbers for this particular tube row.

The plot reinforces the fact that at high flow rates (large Reynold's numbers, Re $\geq$ 20,000), the head loss coefficient is approximately constant, which suggests the data's general form is correct. The plots of the manipulated raw frequency data and the above

discussion suggests that the form of the plotted results is intuitively reasonable, and physically feasible.

3.4   Empirical Models of PRHR Hx Pressure Drop

To characterize the PRHR Hx, it was necessary to be able to determine per tube flow rates. The per tube flow rates can be thought of as the fluid flow split between the eighty-eight PRHR Hx tubes. Fluid will enter the PRHR Hx and then flow through the eighty-eight tubes based on the resistance to flow of each tube. The flow was assumed to split equally between each tube on a mass flow rate basis, but the fluid velocity in each tube was not equal. It was assumed that each physically similar tube in a row has the same flow resistance. The tube length in each row was the same and there are ten rows, labeled A-J. It was therefore necessary to determine the fluid flow (or hydraulic) resistance of each tube, which was grouped for simplicity into the row hydraulic resistance.

To determine the hydraulic resistance it was necessary to analyze the data from the PRHR Hx fluid flow bench test. A model of the total hydraulic resistance (K_{total}) can be determined from the raw data as manipulated into Reynold's number versus pressure drop. The following sections are the explanation of the modeling performed on the PRHR Hx to determine a semi-empirical model for K_{total}. Using the semi-empirical model for K_{total}, a computer code was written to perform an iterative flow split calculation and to determine the PRHR Hx pressure drop.

Finally, the model developed was compared to data acquired in actual tests run on the APEX facility. Specifically APEX test data was compared to the K_{total} model and the results of the computer code. The APEX tests provided data on the response of the PRHR system as a whole and the PRHR Hx as a specific component. A result of the comparison uncertainties in the modeling calculations, computer code and integral system test data will be also discussed.

3.4.1   Initial modeling assumptions

The general Bernoulli equation[6] including form losses for the case when mass flow in equals mass flow out can be written as follows:

$$\left(\frac{1}{A}\right)_t \frac{d\dot{m}}{dt} + \left(p_{out} - p_{in}\right) + \rho g\left(z_{out} - z_{in}\right) + \frac{\dot{m}^2}{2\rho}\left(\frac{1}{A_{out}^2} - \frac{1}{A_{in}^2}\right) + \Delta p_{loss} = 0 \tag{3-3}$$

where:

A_{in} = Inlet Area

A_{out} = Outlet Area

Δp_{loss} = Inlet to Outlet Pressure Drop

$\dot{m}$ = System Mass Flow rate

p_{in} = Inlet Pressure

p_{out} = Outlet Pressure

ρ = Density of water

z_{in} = Inlet Elevation

z_{out} = Outlet Elevation

It was further assumed that:

$$\rho g\left(z_{out} - z_{in}\right) = 0, \text{ entrance and exit are at the same elevation,} \tag{3-4}$$

$$\frac{\dot{m}^2}{2\rho}\left(\frac{1}{A_{out}^2} - \frac{1}{A_{in}^2}\right) = 0, \text{ the entrance and exit areas are the same, and} \tag{3-5}$$

$$\left(\frac{1}{A}\right)_t \frac{d\dot{m}}{dt} = 0, \text{ there is no mass flux in the system.} \tag{3-6}$$

This reduces the Bernoulli equation to:

$$P_{out} - P_{in} + \Delta P_{loss} = 0 \tag{3-7}$$

or rearranged:

$$P_{in} - P_{out} = \Delta P_{loss} \tag{3-8}$$

Hence the difference in inlet to outlet pressure is equivalent to delta pressure across the system, which in turn equates to delta pressure due to total losses (form and frictional). Therefore delta pressure due to total losses can be converted into its components of form loss and frictional loss, which is shown below.

$$\Delta P_{total\ losses} = \Delta P_{losses} = \Delta P_{frictional\ losses} + \Delta P_{form\ losses} \tag{3-9}$$

Each delta pressure component is composed of a head loss coefficient times the fluid velocity and density, over twice the lbm to lbf conversion constant g_c. Below is the expansion of equation (3-9), as stated above:

$$\frac{K_{total\ losses}\rho v^2}{2g_c} = \frac{K_{frictional\ losses}\rho v^2}{2g_c} + \frac{K_{form\ losses}\rho v^2}{2g_c} \tag{3-10}$$

Dividing out the velocity (which is assumed constant) and constant terms (density and g_c) leads to an equation for total head loss coefficient, K_{total} as:

$$K_{total\ losses} = K_{total} = K_{frictional\ losses} + K_{form\ losses} \tag{3-11}$$

3.4.2   Modeling Form Losses

The process of finding K_{total} was broken into two parts, first a value for form losses ($K_{form\ losses}$) was determined and then an expression for frictional losses. An approximation for $K_{form\ losses}$ comes from inspection of the data from the PRHR Hx flow test. A value for K_{total} at each data point was determined using the pressure drop and velocity data, and equation (3-2). A graph of K_{total} versus the Reynold's number (Re), shows that K_{total} approaches a final value at high Re numbers (see Figure 3.14 or Figure 3.23). This final value of K_{total} was approximated as $K_{form\ losses}$ since at high flow rates the frictional losses ($K_{frictional\ losses}$) are negligible, i.e. $K_{frictional\ losses} \ll K_{form\ losses}$. We can assume that $K_{form\ losses}$ for each tube row are equal to the average of the slope of K_{total} versus velocity. Looking at Figure 3.14 or Figure 3.23, $K_{form\ losses}$ can also be seen as the average final value of K_{total} at high Reynold's values.

3.4.3   Modeling Frictional Losses

The second phase of the analysis was a determination of an expression for the frictional losses ($K_{frictional\ losses}$). The friction modeling problem was approached by three methods: an empirical fit of the data with two constants, an empirical fit of the data with one constant, and a empirical fit using a constant and a modified standard equation for laminar friction.

3.4.3.1 Method One, Empirical Fit Model with Two Constants

The first modeling attempt, Method One, was an attempt to model the data as a function of Reynold's number. The model was a fit of the data by numerical approximation and had two coefficients, A_1 and B. The form of this model for the friction term is shown below in the equation for the total head loss coefficient:

$$K_{total} = \left(\frac{A_1}{Re^B} + K_{form\ losses} \right)$$

(3-12)

The model developed in this way (Method One) fits the data well but each row of tubes has two specific empirical constants, Table 3.1. The constant for this model was fit numerically and had too much variation as is shown in Figure 3.25. To avoid the need for so many empirical constants the second method reduced the exponent of the Reynold's number to one.

Tube Row	$K_{form\ loss}$	A_1	B	Coefficient of determination (R^2)
A	10.795	41114.070	1.094	0.989582
B	10.231	49260.218	1.132	0.991864
C	9.591	27259.119	1.046	0.989621
D	9.709	18494.233	1.003	0.993150
E	9.469	27842.797	1.052	0.993425
F	9.207	56429.776	1.153	0.992709
G	8.838	40006.106	1.109	0.994329
H	8.525	18445.314	1.016	0.994339
I	8.418	14792.696	0.990	0.992344
J	8.138	7095.178	0.899	0.994899

Table 3-1   Method One Constants and Coefficient of Determination
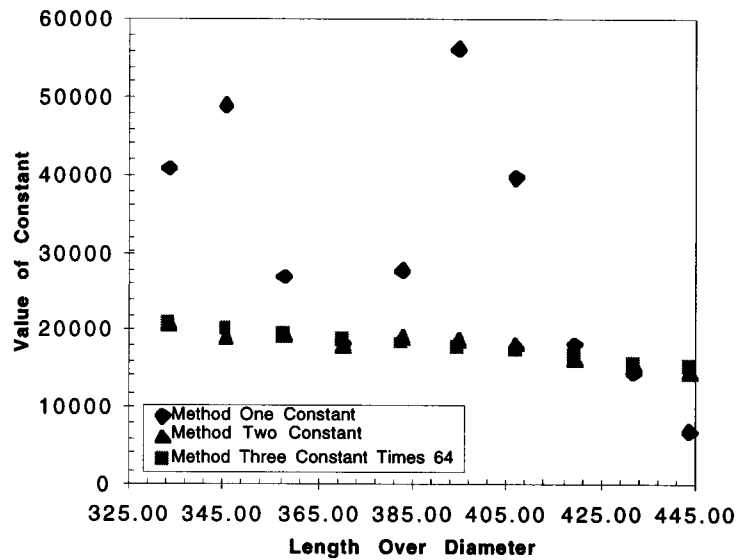
Figure 3.25   Constant A vs. L/D for the Three Models

3.4.3.2   Method Two, Empirical Fit Model with One Constant

Method Two was a simplification of Method One by setting the constant associated with Reynold's number to one, that is, B=1 as shown below:

$$K_{total} = \left(\frac{A_2}{Re} + K_{form\ losses} \right)$$
(3-13)

This approach models the data almost as well as Method One but it still contains a specific constant for each tube row, see Table 3.2. Method Two's constant has less variation than Method one but still was based on numerical approximation, the variation is shown in Figure 3.25.

Tube Row	$K_{form\ loss}$	A_2	Coefficient of Determination (R^2)	L/D
A	10.795	21031.252	0.989137	333.16
B	10.231	19392.976	0.990948	345.41
C	9.591	19605.578	0.989495	357.65
D	9.709	18122.554	0.993149	369.90
E	9.469	19291.618	0.993281	382.14
F	9.207	19102.801	0.991441	394.39
G	8.838	18541.372	0.993675	406.63
H	8.525	16495.876	0.994326	418.88
I	8.418	15840.286	0.992340	431.12
J	8.138	14527.142	0.994269	443.37

Table 3-2   Method Two constants and Coefficient of Determination

3.4.3.3   Method Three, Empirical Fit Using Modified Laminar Friction and One Constant

Method Three was a combination of the Method Two model and a modified standard laminar friction equation, $f_D=64/Re$ (where f_D is equivalent to $K_{friction}$). This approach consisted of finding a line that fit the plot of the Method Two constant versus the L/D of each tube and then using this to modify the standard friction equation. The form of the Method Three model for the friction term is shown below:

$$K_{total} = \left(\frac{A_3 * 64}{Re} + K_{form\ losses} \right) \tag{3-14}$$

The constant A_3 was determined by using a plot of the constant from Method Two versus the pipe ratio (L/D) (see Figure 3.25) and is shown in Table 3-3. This eliminated the use of multiple constants to fit all of the tube rows. Each row has the same

length of pipe (L) and the same diameter (D) over the entire PRHR Hx. As a result, the only variable in the Method Three model was tube length, as given in the fabrication data. Specifically the Method Three constant (A_3) is found to be:

$$A_3 = 578.22 - 0.75705*(L/D) \qquad (3-15)$$

Tube Row	Kform loss	64*A_3	Coefficient of Determination (R^2)
A	10.795	20863.494	0.989122
B	10.231	20270.198	0.990451
C	9.591	19676.902	0.989498
D	9.709	19083.607	0.992509
E	9.469	18490.311	0.992846
F	9.207	17897.015	0.990378
G	8.838	17303.720	0.992479
H	8.525	16710.424	0.994284
I	8.418	16117.128	0.992268
J	8.138	15523.832	0.993234

Table 3-3   Method Three constants and Coefficient of Determination

3.4.4   Model Analysis

All three methods were evaluated based on the statistical parameter called coefficient of determination (R^2). The coefficient of determination is based on an analysis of the residuals, which are the difference between actual data values and modeled values. The sum of the squares of the residuals are compared to the sum of the squares of the

model values through the following equation[7]:

$$\text{Coefficient of Determination (R}^2) = \frac{\sum(\text{Model Values})^2}{\sum(\text{Model Values})^2 + \sum(\text{Residual Values})^2} \quad (3\text{-}16)$$

In the analysis of the models, a coefficient of determination was calculated for each data modeling method. The acceptance criteria were an R^2 larger than 0.98 (no more than 2% deviation from the test data). The coefficients of determination were calculated using equation 3-16 and are presented and discussed below for each of the three modeling methods.

3.4.4.1   Assessment of Method One Model

The model used for Method One was a purely empirical fit so it is based entirely on the data set. A plot of the model's results shows that the model fit the data set well, see Figure 3.14 or Figure 3.23. Because Method One was an empirical fit of the data set, it came very close to predicting the data set, the R^2 range was from .9894 to .9948, see Table 3.1. Statistically this method was the best at predicting, or modeling, the data set, but the model was based entirely on the data set which will not be as useful as a semi-empirical model. Because the model was so heavily based on the data set it's application is limited to the data's range of accuracy and applicability. It is desirable to use to develop a model applicable to other systems.

3.4.4.2   Assessment of Method Two Model

The model used for Method Two was also an empirical fit so it was designed based on the data set. As with the Method One model, Method Two comes very close to predicting the data set, the R^2 range being from .9891 to .9943 (see Table 3.2.) The Method Two model was approaching a semi-empirical model but still relied on specific constants for each row (found by numerical analysis of the data set.) It would be preferable to have an equation based on only physical properties and a empirical factor.

3.4.4.3   Assessment of Method Three Model

This model fit the data very well: the coefficient of determination (R^2) ranged from 0.9891 to 0.9943, a comparison of K_{total} versus Reynold's number revealed that, the model function fit the K_{total} data very closely, as seen in the Figure 3.14 or Figure 3.23. Table 3.4 below summarizes the elements of the Method Three model.

Tube Row	Length/Diameter	Value of Constant A_3	Coefficient of determination (R^2)
A	333.16	20863.493	0.9891
B	345.41	20270.198	0.9905
C	357.65	19676.902	0.9893
D	369.90	19083.607	0.9925
E	382.14	18490.311	0.9928
F	394.39	17897.015	0.9904
G	406.63	17303.719	0.9925
H	418.88	16710.424	0.9943
I	431.12	16117.128	0.9923
J	443.37	15523.832	0.9923

Table 3.4   Values of Constant A_3 for Method Three Model

3.4.4.4   Summary of the model chosen, Method Three

The model chosen, Method Three, is a semi-empirical model developed from the data set that uses only the physical quantity L/D (pipe ratio) and velocity to predict the head loss coefficient. Method Three was chosen because it is semi-empirical and this means that in the future it can be tested as to its applicability to other tube systems. Method three was found to accurately predict the values of the head loss coefficient (K_{total}) for every tube row in the APEX PRHR Hx.

The model for K_{total} chosen was:

$$K_{total} = \left\{ [578.22 - 0.75707(L/D)]\frac{64}{Re} + K_{form\ losses} \right\}$$

(3-17)

The chosen model was based on the respective length of each tube row. Additionally, the model has been tested and fits the data collected from the PRHR Hx flow test with a coefficient of determination of no less than 0.989 (1.1% deviation from test data). The coefficient of determination is therefore within the acceptance range of greater than .98 or less than 2% deviation from test data.

3.5   Comparisons to Pressure Drop Data

The next step was to create a model for the installed PRHR Hx system. The PRHR Hx system was considered to contain all components between the inlet pipe and outlet pipe of the PRHR Hx. Specifically the system was the PRHR Hx the upper (inlet) head, the PRHR Hx, and the PRHR Hx lower (outlet) head. This system was significantly different than the single tube test used to determine the tube model.

To determine the final form of the model for the PRHR Hx, a computer code was written to combine the per tube model into a heat exchanger system model. The code is presented in the following sections. The initial code form was simply the tube flow resistances combined in parallel at the given flow rate. This was found to not be sufficient due to differences in the tube model summed to the in-situ geometry and system components. As a result a modified code was developed which led to a converged code that modeled the PRHR Hx system very well.

3.5.1 Computer Code Development for Passive Residual Heat Removal System Heat Exchanger Flow Split Determination

The next step in the characterization of the PRHR Hx was to create a computer code (program) that could determine the tube flow split given the inlet mass flow rate. The code also calculates the pressure drop across the PRHR Hx. The code was written in FORTRAN and is detailed in the Software Users Manual, PRHRVEL-'Passive Residual Heat Removal Heat Exchanger Tube Velocity'[8]. The code is based on the Method Three model for tube hydraulic resistance.

The first code (PRHRVEL) used the sum of the tubes' resistances in parallel to determine the fluid flow split in each PRHR Hx tube. Once the flow split was determined the PRHR Hx pressure drop could be determined as the sum of the tubes' resistances in parallel. This code method was found to be inferior to the actual in-situ test data as discussed in section 3.5.2, and as a result a modified version that included input of additional form losses was created and called PRHRPLUS. The second code (PRHRPLUS) is identical to the first code except for the addition of a variable to add the additional form loss term.

3.5.1.1 Code Description

The PRHRPLUS code used the Method Three model which was detailed in section 3.4.3.3 of this document. In general, this model is based only on tube length over diameter (L/D_{Tube}) and the Reynold's number of the fluid flowing through it. The model is used to calculate the total hydraulic resistance across the PRHR Hx and the individual tube hydraulic resistance. From tube hydraulic resistances and the total hydraulic resistance the flow split is calculated. The calculation of flow split is an iterative process

but the Method Three model is good enough that the code can converge in only a few iterations.

3.5.1.2   Code Methodology

The general approach of the PRHRPLUS code was to start with an initial tube velocity guess that the flow is evenly split between the tubes. The sum of the tube velocities is the sum of the velocities for each tube row, and is of the form:

$$v_{Inlet} A_{Inlet} = A_{Tube} \left(\begin{array}{c} 6v_A + 8v_B + 10v_C + 10v_D + 10v_E \\ +10v_F + 10v_G + 10v_H + 8v_I + 6v_J \end{array} \right) \qquad (3\text{-}18)$$

The assumption was made that each tube has head loss of the form:

$$h_{L_A} = \frac{v_A^2 k_{T_A}}{2g_c} \qquad (3\text{-}19)$$

Using equation (3-19) with the assumption that head losses across each tube are equal yields the equation below for tube row A's velocity in terms of any other tube row, in this case row B.

$$v_A = v_B \sqrt{\frac{k_{T_B}}{k_{T_A}}} \qquad (3\text{-}20)$$

Now equation (3-18) can be rewritten in the form:

$$v_{Inlet}A_{Inlet} = A_{Tube} \begin{pmatrix} 6v_A + 8v_A\sqrt{\dfrac{k_{T_A}}{k_{T_B}}} + 10v_A\sqrt{\dfrac{k_{T_A}}{k_{T_C}}} + 10v_A\sqrt{\dfrac{k_{T_A}}{k_{T_D}}} \\[2ex] +10v_A\sqrt{\dfrac{k_{T_A}}{k_{T_E}}} + 10v_A\sqrt{\dfrac{k_{T_A}}{k_{T_F}}} + 10v_A\sqrt{\dfrac{k_{T_A}}{k_{T_G}}} \\[2ex] +10v_A\sqrt{\dfrac{k_{T_A}}{k_{T_H}}} + 8v_A\sqrt{\dfrac{k_{T_A}}{k_{T_I}}} + 6v_A\sqrt{\dfrac{k_{T_A}}{k_{T_J}}} \end{pmatrix} \qquad (3\text{-}21)$$

Now solving the above equation for a particular tube row (row A):

$$v_A = \frac{v_{Inlet}A_{Inlet}}{A_{tube}\sqrt{k_{T_A}}\,(X)} \qquad (3\text{-}22)$$

where X is the velocity weighting factor given by:.

$$X = \begin{pmatrix} \dfrac{6}{\sqrt{k_{T_A}}} + \dfrac{8}{\sqrt{k_{T_B}}} + \dfrac{10}{\sqrt{k_{T_C}}} + \dfrac{10}{\sqrt{k_{T_D}}} + \dfrac{10}{\sqrt{k_{T_E}}} \\[2ex] + \dfrac{10}{\sqrt{k_{T_F}}} + \dfrac{10}{\sqrt{k_{T_G}}} + \dfrac{10}{\sqrt{k_{T_H}}} + \dfrac{8}{\sqrt{k_{T_I}}} + \dfrac{6}{\sqrt{k_{T_J}}} \end{pmatrix} \qquad (3\text{-}23)$$

Next the code calculates the head loss coefficients from the initial velocities found as in equation (3-22). The equations for tube head loss coefficient are of the form:

$$K_{total} = \left\{ [578.22 - 0.75707(L/D)]\frac{64}{Re_{tube}} + K_{form\ losses} \right\} \qquad (3\text{-}24)$$

By substituting in the equation for Reynold's number:

$$Re_{tube} = \frac{\rho v_{tube} D_{tube}}{\mu} \qquad (3\text{-}25)$$

The equation for head loss coefficient becomes:

$$K_{total} = \left\{ \frac{[578.22 - 0.75707(L/D)]64}{\dfrac{\rho v_{tube} D_{tube}}{\mu}} + K_{form\ losses} \right\} \qquad (3\text{-}26)$$

The sum of all of the velocity weighting factor (X) is calculated using equation (3-23). Using this weighted sum the code calculates the velocity prime for the tubes using an equation of the form:

$$v'_{tube} = \frac{v_{Inlet} A_{Inlet}}{A_{tube} \sqrt{k_{tube}} (X)} \qquad (3\text{-}27)$$

This process is repeated until there is no significant change between velocity (calculated from equation (3-22)) and velocity prime (calculated from equation (3-27)) for all tubes. This means that the change between velocities and velocity primes are very small, on the order of $(v-v'/v)*100=0.0001$ %.

Once the final velocity of each tube row has been found the results are printed to the screen and an output file that contains the per iteration velocity and velocity primes. A PRHR Hx total pressure drop is also calculated based on the sum of the tube hydraulic resistances summed in parallel. The equation for pressure drop is:

$$\Delta P = \frac{K_{Total} \rho v_{inlet}^2}{2g_c} \qquad (3\text{-}28)$$

where K_{total} is calculated using:

$$K_{Total} = \left(\left(\begin{array}{c} \left(\dfrac{6}{k_{T_A}} + \dfrac{8}{k_{T_B}} + \dfrac{10}{k_{T_C}} + \dfrac{10}{k_{T_D}} + \dfrac{10}{k_{T_E}} \right. \\ \left. + \dfrac{10}{k_{T_F}} + \dfrac{10}{k_{T_G}} + \dfrac{10}{k_{T_H}} + \dfrac{8}{k_{T_I}} + \dfrac{6}{k_{T_J}} \right)^{-1} \\ + K_{additional} \end{array} \right) \right)$$

(3-29)

where $K_{additional}$ is the additional form losses needed to model the PRHR Hx as a system. Figure 3.26 shows the value of K_{total} for the whole system based on a per tube Reynolds number calculated from the data set with and with out the $K_{additional}$ form losses. As a further check the PRHR Hx inlet velocity is also calculated from equation (3-18) and output. The output is written to a file called PRHRVEL.OUT (or PRHRPLUS.OUT).
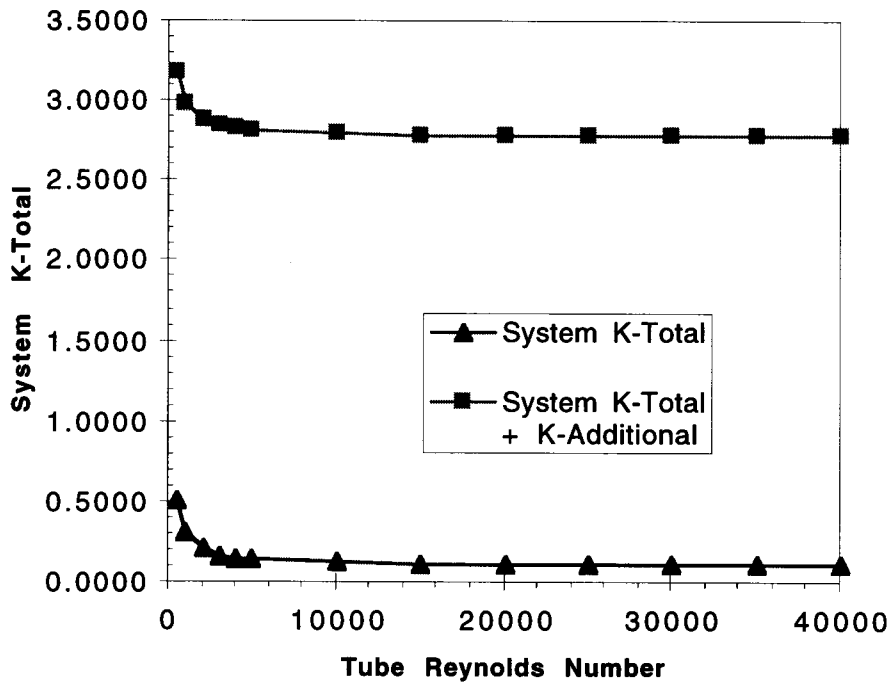
Figure 3.26   System K_{total} vs. Tube Reynold's Number

3.5.2 Comparison of Tube Model & Heat Exchanger Computer Code to Specific Passive Residual Heat Removal System In-Situ Test Data from the Oregon State University APEX Plant

The main difference between the bench test and the as built PRHR Hx comes from the fact that the eighty-eight tubes are welded to inlet and outlet header plates an the inlet and outlet headers. The header plates increase the surface area and hence will increase fluid resistance. The inlet and outlet heads of the PRHR Hx induce additional flow resistance effects as well.

To model the in-situ PRHR Hx system a fluid flow test was performed. The in-situ PRHR Hx system fluid flow low test was performed on the PRHR Hx as installed in the APEX Test facility. A description of the in-situ test is presented in section 3.5.2.1

3.5.2.1 Test Description

The test was performed by varying flow rates through the PRHR Hx by means of regulating the flow output of the reactor coolant pumps. Pressure drop across the PRHR Hx was measured by a delta pressure cell with pressure taps at the PRHR Hx inlet and outlet heads. Data was acquired using the APEX Test facilities Data Acquisition System (DAS). The DAS sampled the flow and pressure drop readings on an eight second interval continuously for the duration of the test (approximately 2000 seconds).

The test procedure was to start with zero flow and then increase reactor coolant pump output in approximately one gallon per minute (GPM) steps. The flow rate was maintained for approximately 45 seconds at each step while pressure drop was recorded by the DAS. In this way flow was increased from zero to almost 16 GPM and then decreased back to zero. The data taken is plotted in Figure 3.27.
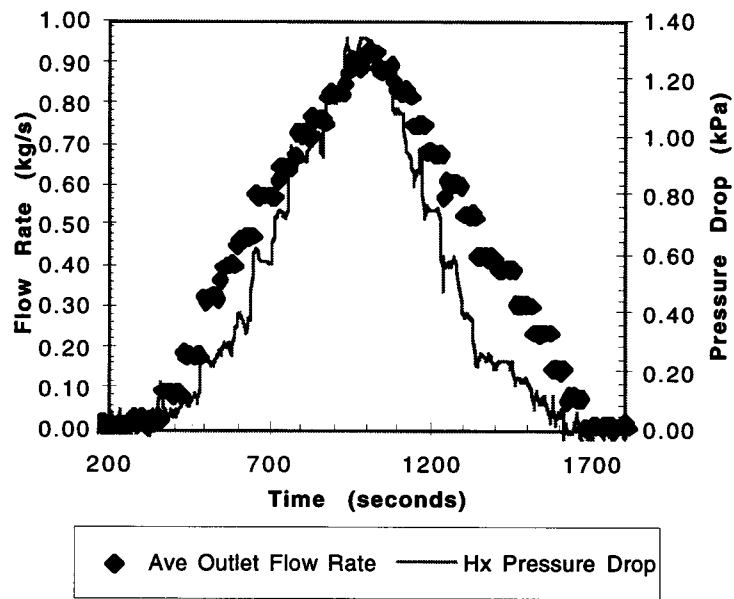
Figure 3.27   Data Taken During In-Situ PRHR Hx Flow Test

In the flow test the PRHR Hx was isolated from other plant systems and the IRWST tank was kept at an approximately constant temperature of 100 °F. The IRWST was still warm due to residual heat from a previous test. This was acceptable and was taken in to account in all analyses.

3.5.2.2   Test Results

The in-situ PRHR Hx flow test was performed successfully. Figure 3.28 presents the pressure drop versus velocity squared. This figure shows a linear relationship as one would expect for such a fluid flow test.
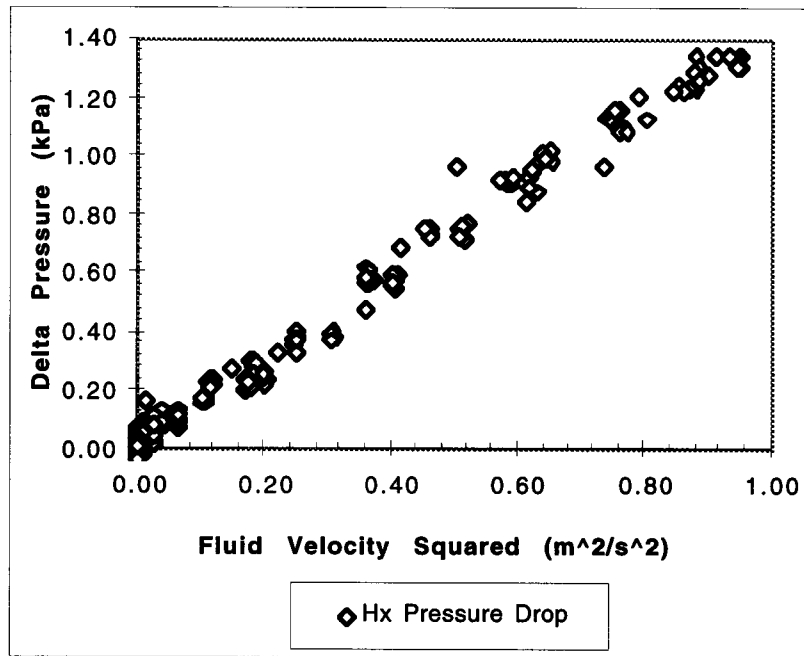
Figure 3.28   DP vs. Velocity Squared for In-Situ PRHR Hx Flow Test

As seen in Figure 3.28 a slope which is analogous to the form loss coefficient (K_{Total}) was determined for the PRHR Hx system. The value of PRHR Hx system K_{Total} was compared to several executions of the modified the computer code (see section 3.5.1) developed for the PRHR Hx, see Figure 3.29. It was noted that additional form loss of 2.675 was determined to be necessary to bring the code in line with the experimental data taken for the PRHR Hx system. An R^2 for several code runs with additional from losses were determined and are presented below in Table 3.5.
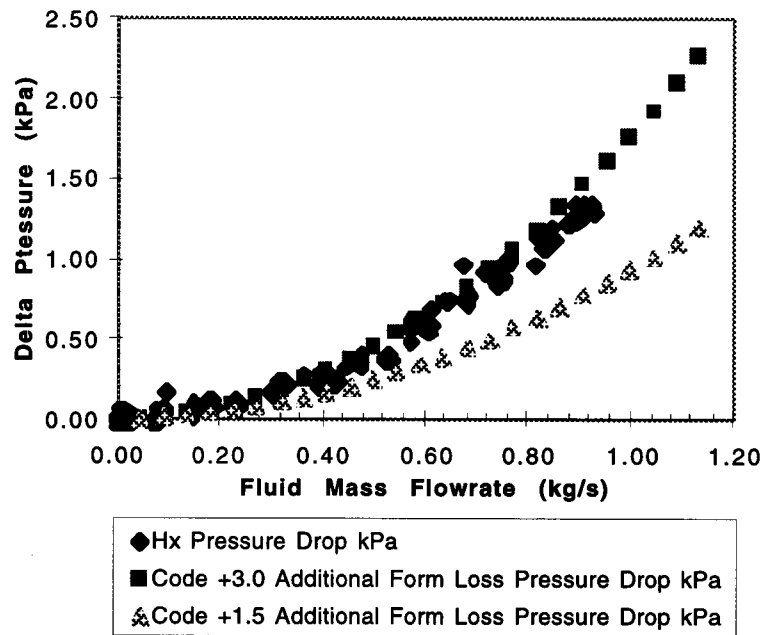
Figure 3.29 DP vs. Mass Flow rate for In-Situ PRHR Hx Flow Test and Code with
Additional Form Losses

Additional From Loss	+ 2.600	+ 2.625	+ 2.650	+ 2.675	+ 2.700	+ 2.750
Coefficient of determination (R^2)	0.9939	0.9942	0.9944	0.9945	0.9944	0.9725

Table 3.5   Results of Additional Form Losses on PRHR Hx System Code

The best coefficient of determination came from adding 2.675 to the form losses
calculated by the PRHR Hx system code. The R^2 was .9945 which leads to a deviation of
less than one percent, an acceptable deviation in this case.

3.5.3   Data Uncertainties in Model, Code, & In-Situ Test Data

The model and code developed to model the PRHR Hx system have certain inherent uncertainties which are tied to the experimental data on which they are based. To get an accurate idea of the uncertainty involved one must first look at the experimental data collected. The data initially collected for the per tube PRHR Hx model was collected using calibrated instruments that are tested for accuracy and within the manufacturers specifications during operation. Similarly the instruments used during the PRHR Hx system in-situ test were calibrated, tested for accuracy, and within the manufacturers specifications during operation.

To determine the possible uncertainties in the data, a study of the instruments used in the data collection was performed using the manufacturers stated accuracy for each device. The three main instrument types used in testing were two different fluid flow meters and two similar but differently ranged delta pressure sensors. The delta pressure (DP) cells used function identically except for their ranges and are accurate within ±1%. The DP cells are calibrated by certified technicians on a regular basis at the APEX Test Facility.

The testing of the PRHR Hx system used flow meters of two different types. The first type of flow meter used was the frequency counting type. Frequency counting flow meters determine flow by frequency output which can be directly related to fluid velocity. Two frequency type flow meters were used in testing individual PRHR Hx tubes and were both calibrated to be accurate within ±1%. The second flow meter measured in volumetric units (gallons per minute or GPM), which was calibrated by certified technicians on a regular basis at the APEX Test Facility and is known to read within ±1% as well.

The conclusion is therefore that the data values collected are representational of the actual phenomena within an acceptance criteria of ±1%. The effect of instrument inaccuracies was assumed to not have an effect on the overall data trends which are the basis for the model development. The data collected also was numerous so statistical models applied to them are valid within the range of the data values.

3.6   Summary of PRHR Hx Flow Study Findings

The PRHR Hx system flow study showed that the initial tube model successfully modeled the PRHR Hx system if slightly modified. The model was successfully modified with additional form losses and applied in computer code form to the in-situ test data. Inspection of Figure 3.29 shows that the modified model accurately predicts the pressure drop given an inlet flow rate.

3.6.1   Chosen Model for PRHR Hx Tube Simulation

As seen in sections 3.4 and 3.5, a model for best modeling the PRHR Hx system has been determined. The model is based on an empirical relation that comes from experimental tests. The model was developed from theory and has reasonable physical sense as to it's dependence on length over diameter for frictional losses and the use of Reynold's number. The model can be seen in Equation 3-30 below which is identical to equation (3-23).

$$K_{total} = \left\{ [578.22 - 0.75707(L/D)] \frac{64}{Re_{tube}} + K_{form\ losses} \right\} \qquad (3\text{-}30)$$

The model is used in conjunction with an additional form loss of 2.675, which was experimentally determined, to accurately model the PRHR Hx system as built in the APEX Test Facility.

3.6.2   Summary & Conclusions on Flow Test Findings

All of the objectives for the first portion of the study of the PRHR Hx system were achieved.   A bench flow test of the PRHR Hx to obtain a data set of pressure drop across the heat exchanger at various fluid flow rates was performed. A model for the hydraulic resistance of the heat exchanger using the bench test data along with data from an in-situ test of the PRHR Hx system was developed and tested.

Additionally a computer code was developed which can both model the PRHR Hx system pressure drop and determine the flow split of the PRHR Hx system. The computer code was tested and it is accurate within ±1% for PRHR Hx system flows in the range from 0 to 16 GPM.

The ground work has been laid for the further study of the PRHR Hx system as a device for heat rejection. It now remains to apply the model of the PRHR Hx system to actual APEX Test Facility data in order to understand it's capability for heat rejection.

4.   Thermal Characterization of the PRHR Hx

The next phase of analysis is the development of an overall heat transfer coefficient for the PRHR Hx. To characterize the PRHR Hx, it was necessary to compile as much data as possible of the PRHR Hx in operation. The data base was compiled from several APEX tests. The data needed in the data base was PRHR Hx inlet and outlet temperature, IRWST elevational temperature, fluid flow rate, and the total surface area of the Heat Exchanger. All of this data was needed on a interval time basis for each test to be analyzed. The method of tabulation used was an inclusive spreadsheet created in Microsoft™ Excel.

4.1   Theoretical Heat Transfer Models

The PRHR Hx heat removal was studied using an overall heat transfer coefficient. The overall heat transfer coefficient was found using Newton's Law of Cooling[9]. To use Newton's Law of Cooling, the PRHR Hx heat rejection was determined using an energy balance.

4.1.1 Energy Balance

The methodology of the actual heat transfer analysis was based on the energy equation reduced for this specific case. The general energy equation[10] is shown in equation 4-1 below.

$$\frac{\delta Q}{\partial t} - \frac{\delta W_S}{\partial t} = \iint_{cs} \rho \left(e + \frac{P}{\rho} \right)(\vec{v} \bullet \vec{n})dA + \frac{\partial}{\partial t} \iiint_{cv} \rho e dV + \frac{\delta W_\mu}{\partial t} \qquad (4\text{-}1)$$

Assumptions made:

• steady state $\therefore \dfrac{\partial}{\partial t} \iiint_{cv} \rho e dV = 0$

• neglect the friction term $\therefore \dfrac{\delta W_\mu}{\partial t} = 0$

• no work into the system $\therefore \dfrac{\delta W_S}{\partial t} = 0$

This reduces equation (4-1) to:

$$\frac{\delta Q}{\partial t} = \iint_{cs} \rho \left(e + \frac{P}{\rho} \right)(\vec{v} \bullet \vec{n})dA \qquad (4\text{-}2)$$

where:

$\dfrac{\delta Q}{\partial t}$ = the heat rejected by the system

$\iint_{cs} \rho \left(e + \dfrac{P}{\rho} \right)(\vec{v} \bullet \vec{n})dA$ = an integral over the control surface

Equation (4-2) can be integrated at the inlet and outlet and expanded to:

$$\frac{\delta Q}{\partial t} = \left(\frac{v_{out}^2}{2} + gz_{out} + u_{out} + \frac{P_{out}}{\rho_{out}} \right)\rho_{out}v_{out}A_{out}$$

$$- \left(\frac{v_{in}^2}{2} + gz_{in} + u_{in} + \frac{P_{in}}{\rho_{in}} \right)\rho_{in}v_{in}A_{in} \qquad (4\text{-}3)$$

where the energy term e was expanded to $\dfrac{v^2}{2} + gz + u$

We know that:

• $A_{in} = A_{out}$ which can be called A,

• it is assumed that at steady state $v_{in} = v_{out}$ which can be called v,

• from continuity $\dot{m}_{out} = \dot{m}_{in}$ so $\rho_{in} v_{in} A_{in} = \rho_{out} v_{out} A_{out}$ and can be called simply

$\dot{m}$.

Enthalpy is defined by $h = u + P/\rho$ and can be substituted into equation (4-3). With no accumulation of mass, constant area, and a steady state velocity equation (4-3) can be written as:

$$\frac{\delta Q}{\partial t} = \left[\left(gz_{out} + h_{out}\right) - \left(gz_{in} + h_{in}\right)\right]\dot{m} \qquad (4-4)$$

The contribution by the gravitational head is small and the pressure drop will be dealt with later this leads to equation (4-5).

$$\frac{\delta Q}{\partial t} = \left(h_{out} - h_{in}\right)\dot{m} \qquad (4-5)$$

The change in enthalpy $h_{out}-h_{in}$ can be written as $Cp_{ave}\Delta T$[11]. Cp_{ave} is the average of the specific heat evaluated at inlet and outlet temperature and ΔT is $T_{out}-T_{in}$. The final form of the energy equation used was that shown below in equation (4-6).

$$\frac{\delta Q}{\partial t} = \dot{m} Cp_{ave}\Delta T \qquad (4-6)$$

4.1.2 Overall Heat Transfer Coefficient Modeling

Using Newton's Law of Cooling and the overall heat transfer coefficient is a well established method used in industry and has many practical applications. The nature of the approximation is fairly coarse but it can be used over wide ranges of flow conditions as long as the necessary experimental work has been done to properly characterize the heat exchanger used. It is also possible to roughly calculate with known heat transfer correlations and geometry, values of the overall heat transfer coefficient for heat exchangers prior to construction. As always one must know the expected operating conditions for the heat exchanger for U to be of any practical use.

Newton's Law of Cooling states that the energy rejected by an object due to convection is equivalent to some convective heat transfer coefficient times the surface area of the object times the temperature difference between the object and the surrounding medium. The equation is shown below:

$$\dot{Q} = hA\Delta T \tag{4-7}$$

where; $\dot{Q}$ is the energy rejected, h is the convective heat transfer coefficient, A is the object's surface area, and ΔT is the temperature difference.

The general case of Newton's Law of Cooling has been modified for use in heat exchangers by the introduction of an overall heat transfer coefficient called U. U represents all of the heat transfer mechanisms involved. U is a combination of convection inside the heat exchanger tubes, the conduction through the walls, and the convection on

the outside of the tubes. An expansion of U into its various terms is shown below[12]:

$$\frac{1}{U} = \frac{1}{h_o} + R_{fo} + \left[\frac{A_o \ln\left(\frac{r_o}{r}\right)}{2\pi k_w L}\right] + R_{fi}\frac{A_o}{A_i} + \frac{1}{h_i}\frac{A_o}{A_i}$$

(4-8)

In the above equation:

h_o = The outside convective heat transfer coefficient.

h_i = The inside convective heat transfer coefficient.

R_{fo} = The resistance due to fouling on the outside.

R_{fi} = The resistance due to fouling on the outside.

r_o = The outer tube radius.

r_o = The outer tube radius.

A_o = The wall outside area.

A_i = The wall inside area.

k_w = The wall thermal conductivity.

L = The tube length.

As one may note U will vary over the length of the heat exchanger due to temperature differences and will also vary over time due to tube fouling.

In general, U is an experimentally determined factor that is specific to each system tested due to constraints of geometry, construction, materials, and age. Length dependent U's are possible so it is common for U to be averaged for the entire system length. In this document U will be length averaged. U as applied to Newton's Law of Cooling is shown in the equation below[13], which is a modified version of equation (4-7).

$$Q = UA\Delta T_{LMTD}$$

(4-9)

In the equation above ΔT_{LMTD} is the log mean temperature difference which uses the inlet and outlet temperatures in the heat exchanger as well as the inlet and outlet temperatures of the surrounding fluid. The equation for log mean temperature difference is shown below[14].

$$\Delta T_{LMTD} = \frac{(T_1 - t_2) - (T_2 - t_1)}{\ln\left[(T_1 - t_2)/(T_2 - t_1)\right]}$$

(4-10)

The temperatures are: T_1= heat exchanger inlet temperature, T_2= heat exchanger outlet temperature, t_1= surrounding fluid inlet temperature, t_2= surrounding fluid outlet temperature.

4.2 Test Results

The modeling of the PRHR Hx heat transfer was accomplished using the data from eight separate tests. The first six tests are three identical pairs with either forced or natural circulation flow. These tests were part of the integral systems testing[15] performed at the OSU APEX facility. The next two tests were performed as part of a contract with the US NRC.

4.2.1 Description of Integral System Test

The integral systems tests were performed after construction of the OSU APEX facility. The tests were performed to characterize system performance and to perform a "shake-down" or functionality test. The Integral System Tests consisted of several

different testing steps with several different test objectives. The tests that pertain to the PRHR Hx consist of steady state plant operation at varying power levels with either forced flow or natural circulation with the IRWST isolated and not injecting into the primary system.

The specific test of interest HS01 (Hot Shakedown #1) steps 14.32, 14.42, 14.52, 16.16, 16.26, and 16.36. The first three tests (steps 14.32, 14.42, and 14.52) were performed using natural circulation at power levels of 300 kW, 500 kW, and 600kW respectively. The second three tests (steps 16.16, 16.26, and 16.36) were performed under forced flow conditions at the same three power levels (300 kW, 500 kW, and 600kW). The relevant data channels from these tests were extracted from raw data files and compiled in the spreadsheet used.

4.2.2   Description of NRC Tests

The two NRC tests were numbered NRC -5001[16] and NRC-5105[17] and were both natural circulation tests of the OSU APEX plant. The tests fulfill the same criteria as the hot shakedown tests namely that the inlet to the PRHR Hx is single phase fluid and that the IRWST is isolated and not injecting. As before, relevant data channels from these tests were extracted from raw data files and compiled in the spreadsheet used.

4.3   Comparisons to Heat Transfer Data

The energy equation above was applied to each test data set to determine the heat rejection. The plots in Figures 4.1-4.8 show the results of the energy equation application. An average value of both heat rejection and flow rate were needed for the

next phase of data analysis. The averages were taken from the data set as eight sets of heat rejection versus outlet Reynold's number, one for each test. This was done to ensure that the steady state assumption was applicable. Figure 4.9 summarizes the heat rejection analysis results. Reynold's Number (Re) is defined as $Re = \frac{\rho v D}{\mu}$ where ρ is the fluid density, v is the fluid velocity, D is the PRHR Hx outlet tube diameter, and μ is the fluid viscosity.
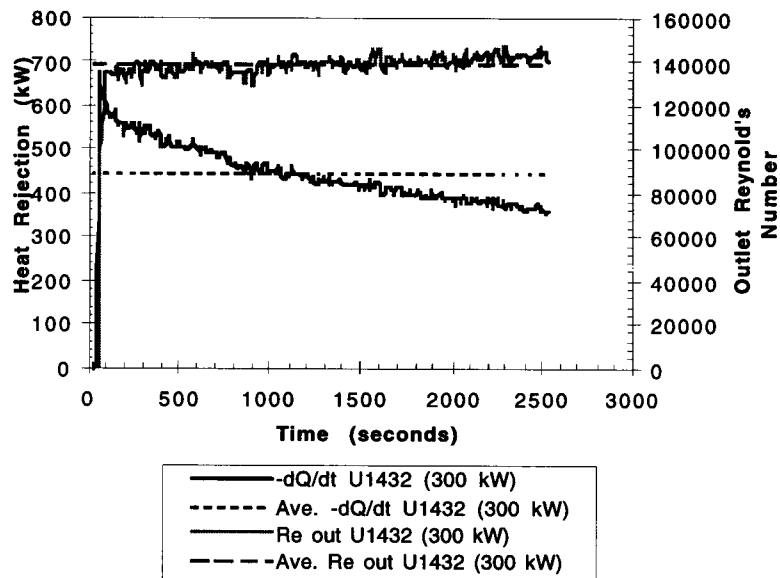
Figure 4.1   Heat Rejection and Outlet Reynold's Number vs. Time for HS01 Step U1432
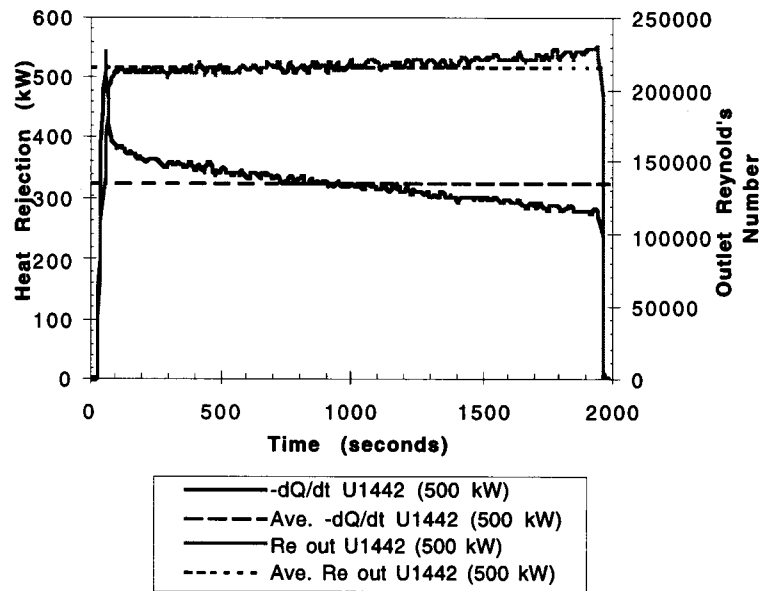
Figure 4.2   Heat Rejection and Outlet Reynold's Number vs. Time for HS01 Step
U1442
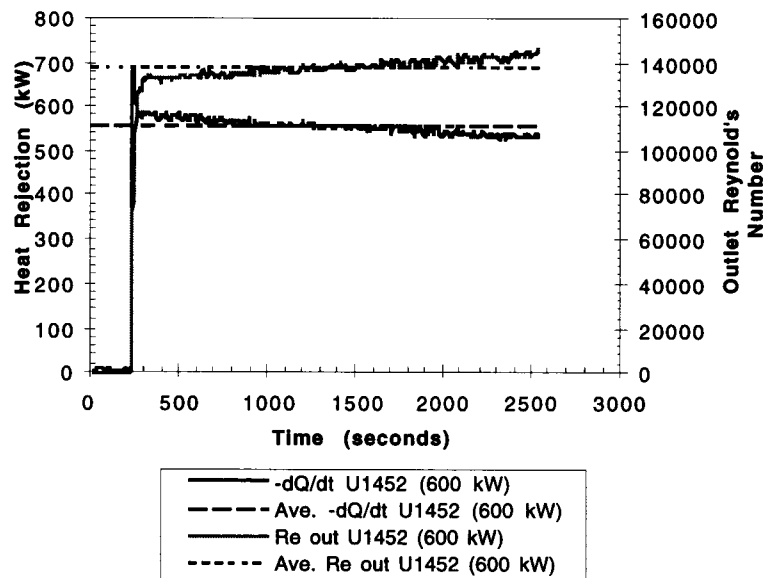
Figure 4.3   Heat Rejection and Outlet Reynold's Number vs. Time for HS01 Step
U1452

Figure 4.4   Heat Rejection and Outlet Reynold's Number vs. Time for HS01 Step U1616

Figure 4.5   Heat Rejection and Outlet Reynold's Number vs. Time for HS01 Step U1626
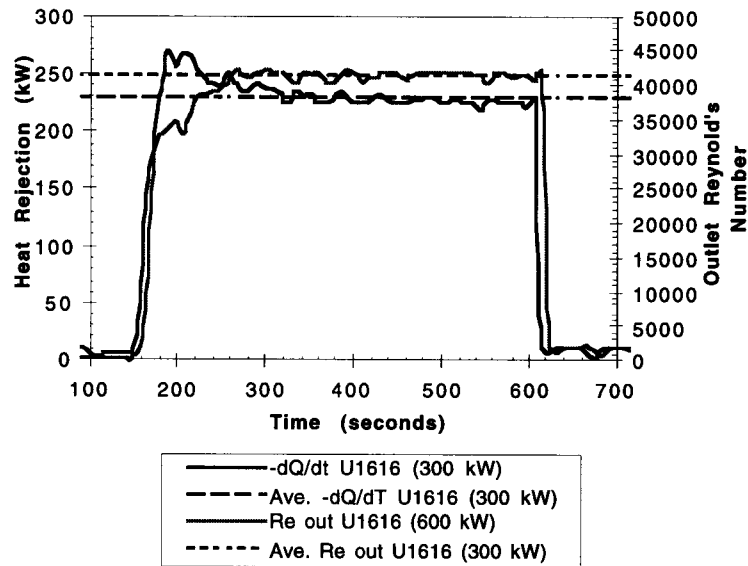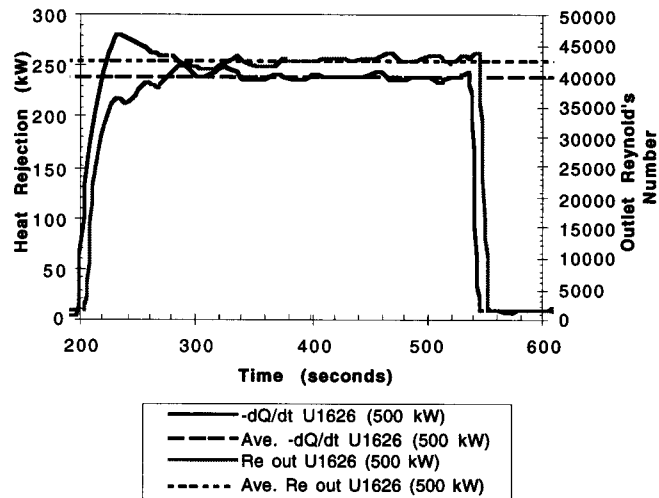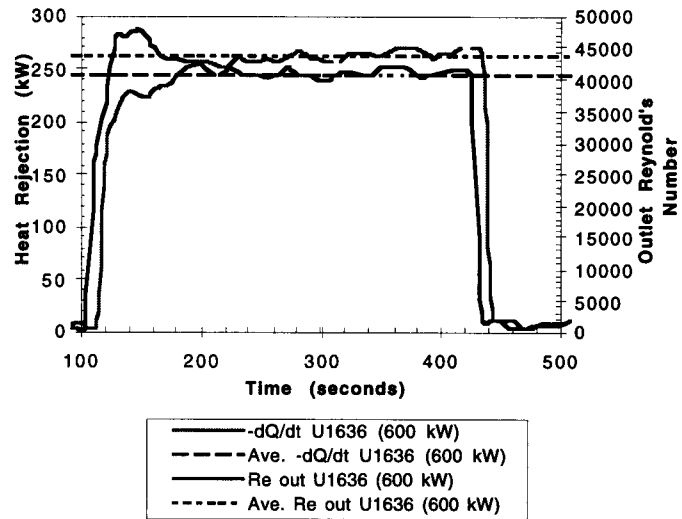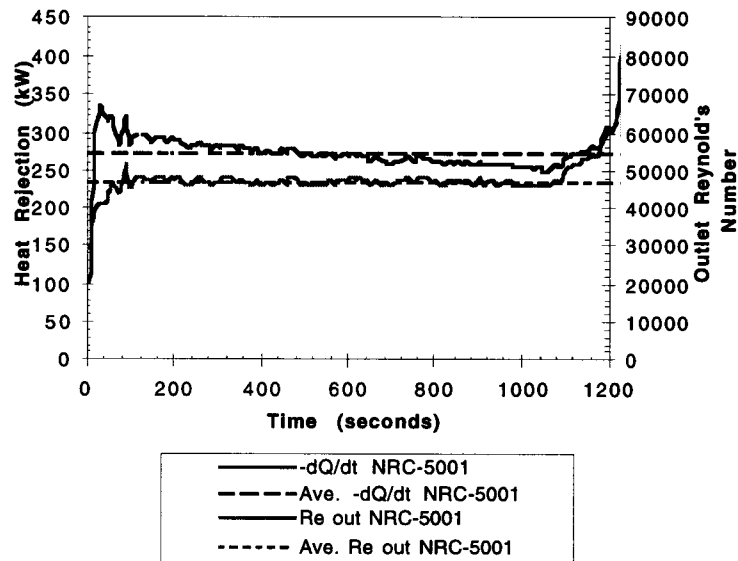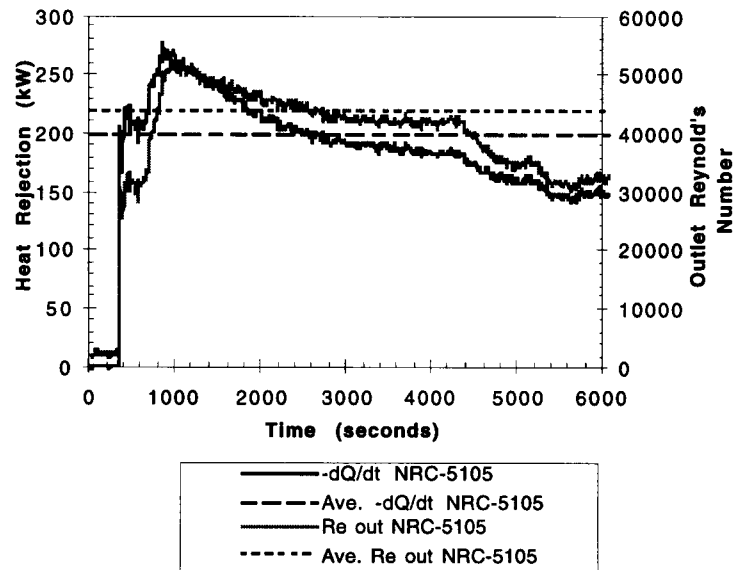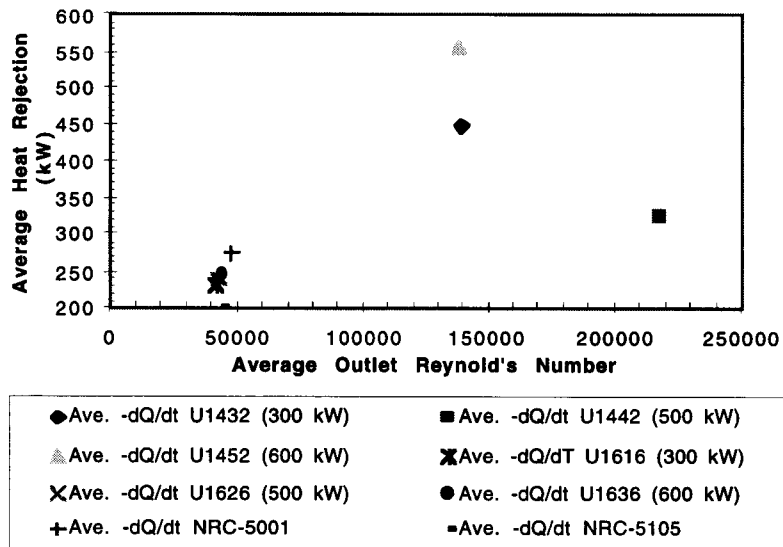
Figure 4.6   Heat Rejection and Outlet Reynold's Number vs. Time for HS01 Step U1636

Figure 4.7   Heat Rejection and Outlet Reynold's Number vs. Time for NRC-5001

Figure 4.8   Heat Rejection and Outlet Reynold's Number vs. Time for NRC-5105

Figure 4.9   Average Heat Rejection vs. Average Outlet Reynold's Number

Knowing the heat rejection from each test allowed an overall heat transfer coefficient to be developed for each test. The model used for the overall heat transfer coefficient comes from equation (4-9) solved for U as shown below:

$$U = \frac{\dot{Q}}{A \Delta T_{LMTD}}$$

(4-10)

The results of the application of the above equation to each test are shown in Figures 4.10 through 4.15. The results of the application of equation (4-10) to the two NRC tests are shown in Figures 4.16 and 4.17. As with the heat rejection calculations the overall heat transfer coefficients were also averaged.
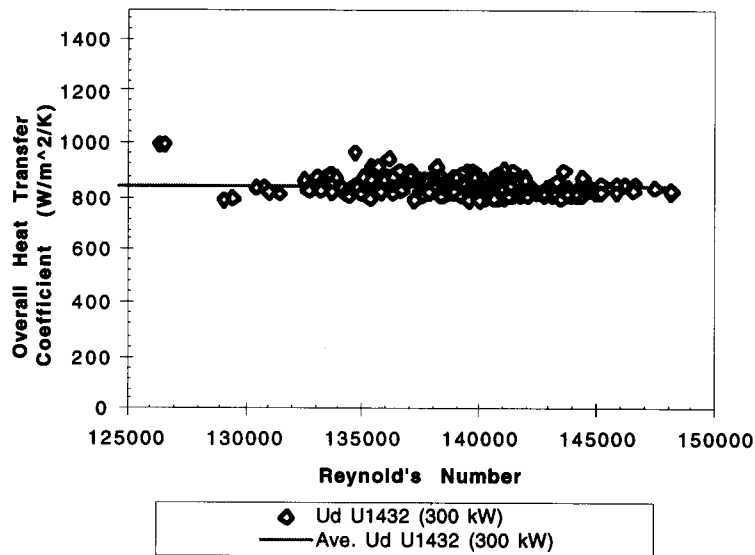
Figure 4.10 Heat Transfer Coefficient vs. Outlet Reynold's Number for HS01 Step U1432
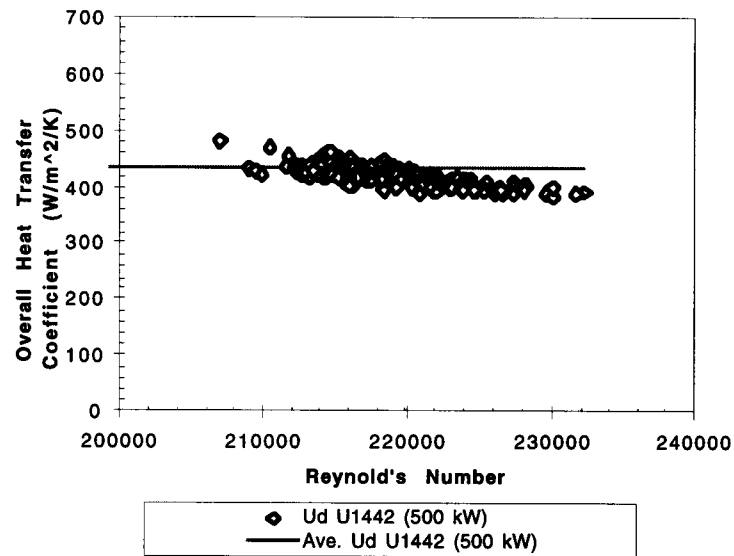
Figure 4.11   Heat Transfer Coefficient vs. Outlet Reynold's Number for HS01 Step
U1442
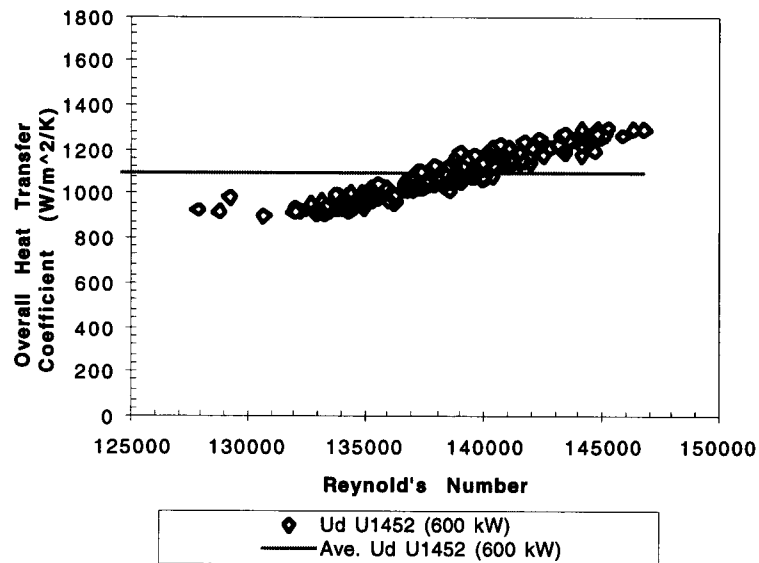
Figure 4.12   Heat Transfer Coefficient vs. Outlet Reynold's Number for HS01 Step
U1452
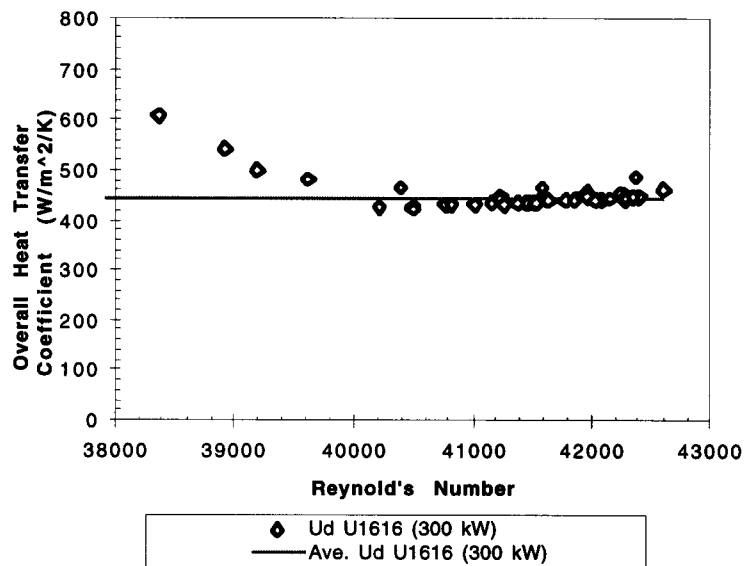
Figure 4.13   Heat Transfer Coefficient vs. Outlet Reynold's Number for HS01 Step
U1616
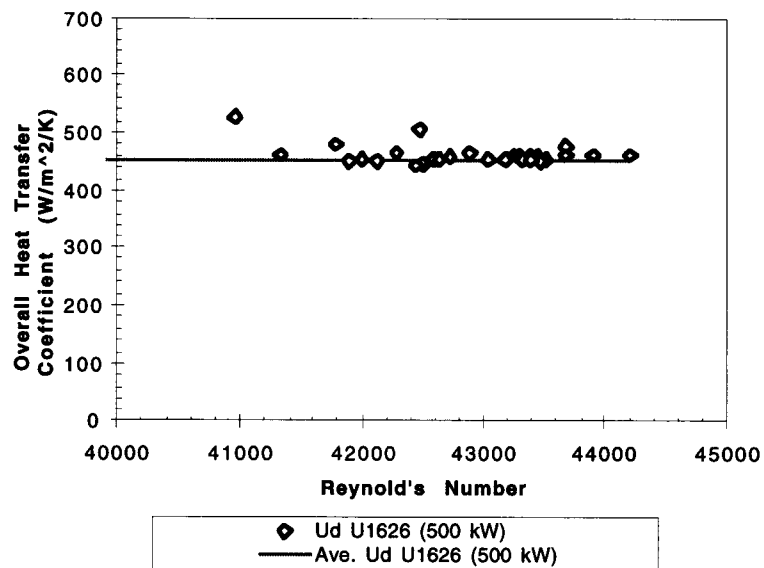
Figure 4.14   Heat Transfer Coefficient vs. Outlet Reynold's Number for HS01 Step
U1626
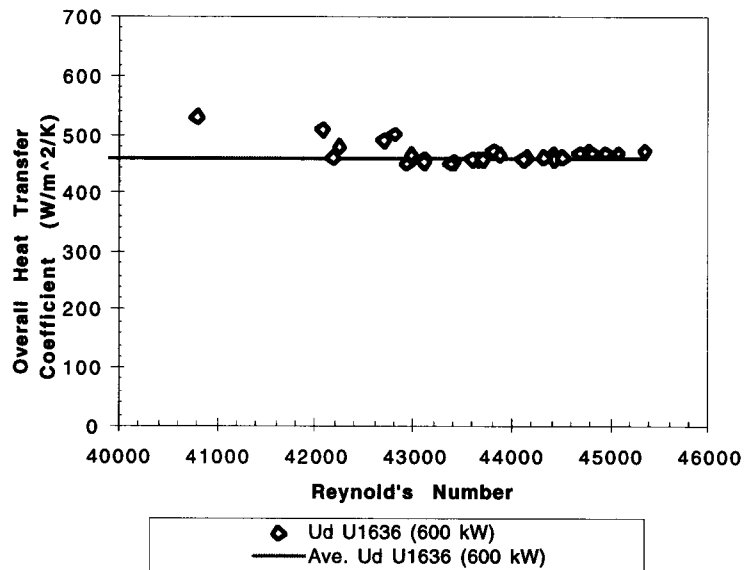
Figure 4.15 Heat Transfer Coefficient vs. Outlet Reynold's Number for HS01 Step U1636
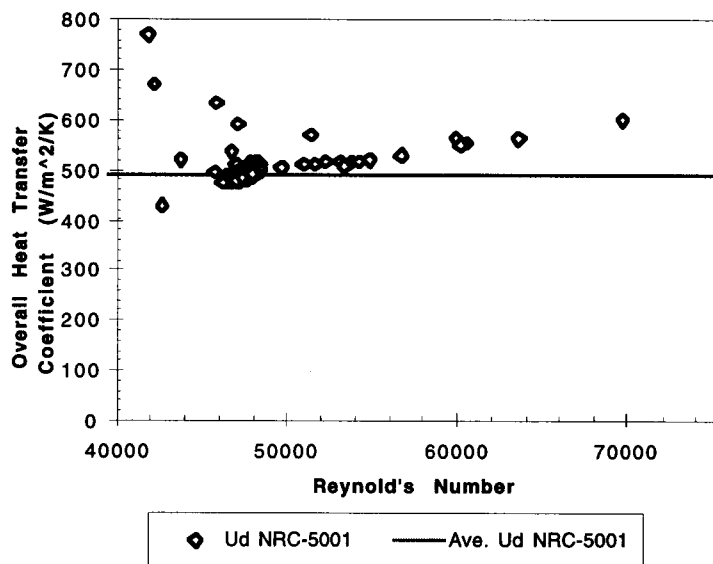
Figure 4.16 Heat Transfer Coefficient vs. Outlet Reynold's Number for NRC-5001
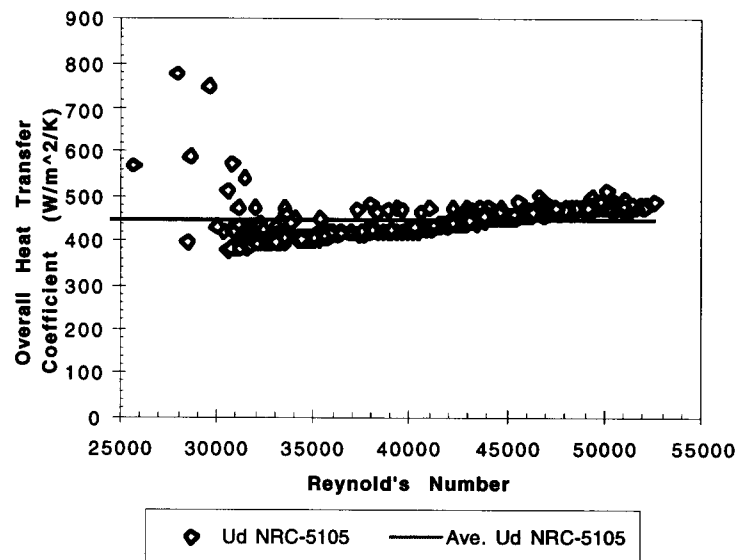
Figure 4.17   Heat Transfer Coefficient vs. Outlet Reynold's Number for NRC-5105

The results of the heat transfer calculations were eight data points of overall heat transfer coefficient versus outlet Reynold's number. Figure 4.18 shows a plot of the eight data points resulting from the heat transfer calculations.
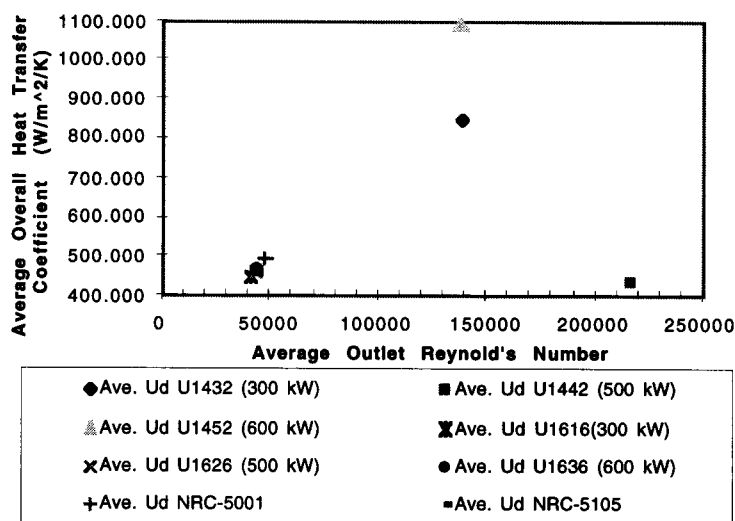
Figure 4.18 Average Heat Transfer Coefficient vs. Average Outlet Reynold's Number

4.4 Conclusions of Heat Transfer Analysis

A database of PRHR Hx heat rejection capability for several different cases was created. The database was used to study the PRHR Hx in both natural circulation and forced flow. The heat rejection calculations performed give insight into the PRHR Hx's function in a variety of conditions. The results of the heat rejection analyses were used to find U for the PRHR HX in different conditions.

The results of the U analysis are:

- For the forced flow tests the value of U for the PRHR Hx is ~450 W/m^{2}K.

- The core power level does not have any discernible effect on the overall heat transfer coefficient in the case of forced flow.

- The natural convection cases appear to have no pattern for U as a function of Reynold's Number.

- There are other phenomena involved in PRHR Hx heat rejection ability and overall heat transfer that need to be investigated.

5.   Evaluation of Station Blackout

One of the tests performed in APEX was NRC-5002[18], a station blackout simulation. For this scenario, it was assumed that station power is lost causing the reactor coolant pumps to trip. The controls rods are immediately inserted and the primary system transitions from a forced flow condition to a natural circulation mode of operation. The PRHR system is actuated to remove decay power from the core for a prolonged period of time until the Automatic Depressurization System (ADS) is actuated.

5.1   Description of the APEX Station Blackout Tests (NRC-5002 & NRC-5102)

Test NRC -5002 (and NRC-5102[19]) was initiated at a core power level of 425 kW. Test NRC-5102 was a re-test of NRC-5002 and was identical except that the test ran for approximately 7 hours. The primary coolant was initially at a pressure of 2.76 MPA (400 psia) and a hot leg temperature of 204 C (420 F). The PRHR was initially isolated and the IRWST was liquid full and at ambient temperature. Upon a simulated loss of station power, the reactor coolant pumps were tripped, the core power placed into decay mode and the primary system transitioned to a natural circulation mode of core cooling. As the steam generators removed core power, they experienced a cyclic secondary side pressure relief process. This continued until the PRHR system was actuated to remove the core decay power.

The PRHR system was permitted to operate for 5 hours for NRC-5002 and 7 hours for NRC-5102. During this period, heat was transferred from the core to the IRWST liquid. As shown in Figures 5.1 and 5.2, the fluid temperature measurements along the vertical axis of the IRWST indicated that the fluid became thermally stratified.

Eventually the liquid at the top of the IRWST reached saturation conditions. As the test progressed, the saturation layer grew towards the bottom of the IRWST altering the PRHR Hx's heat rejection process. Eventually, all of the IRWST liquid, except the liquid layer below the heat exchanger, reached saturation conditions.
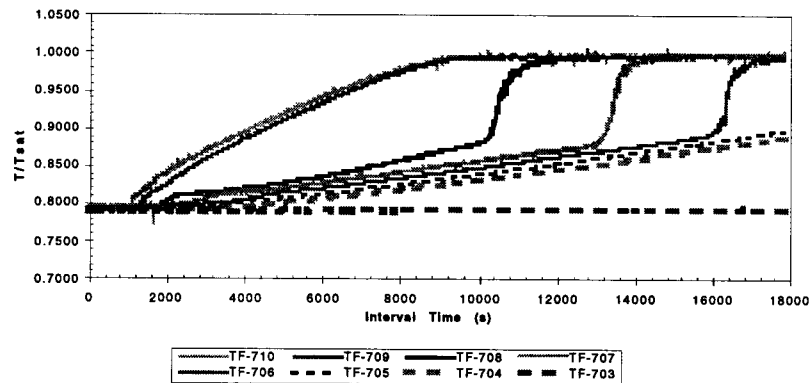
Figure 5.1   IRWST Elevational Temperature Fractions (NRC-5002)
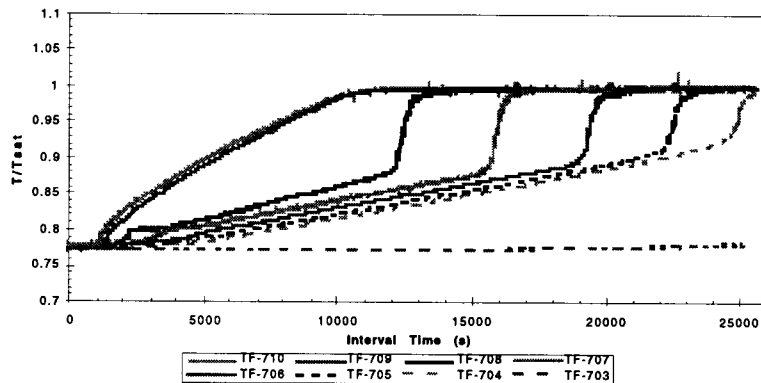
Figure 5.2   IRWST Elevational Temperature Fractions (NRC-5102)

5.2 Description of PRHR Hx Heat Rejection

The following simple energy balance can be used to determine the total amount of heat rejected by the PRHR Hx:

$$\frac{\delta Q}{\partial t} = \dot{m} Cp_{ave} \Delta T \tag{5-1}$$

where $\dot{m}$ represents the mass flow rate of fluid through the heat exchanger, Cp_{ave} is the average specific heat at constant pressure, ΔT is outlet to inlet fluid temperature difference, and the heat rejection rate by dQ/dt. Equation (5-1) assumes steady-state conditions, with no shaft work and negligible gravitational and friction energy terms.

In addition to finding the total heat rejected by the PRHR Hx, the heat rejected by the horizontal and vertical sections of the heat exchanger were also determined. As shown in Figure 2.4, the PRHR Hx can be divided into four zones based on the locations of the available instrumentation. Zone 1 is the upper horizontal section from inlet to just before the tube bend. Zone 2 is the upper vertical section including the upper bend down to the PRHR Hx midpoint. Zone 3 is the mirror image of zone 2 including the vertical tube running from PRHR Hx midpoint down to and including the bend. Zone 4 is the lower horizontal section from the end of the bend to the PRHR Hx outlet. Both inlet and outlet zones (1 and 4) include the PRHR inlet and outlet plena.

The results of the application of the energy equation can be better used as a ratio of heat rejection for a zone divided by total heat rejection for the PRHR Hx or:

$$\frac{\delta Q / dt_{zone}}{\delta Q / dt_{system}} \tag{5-2}$$

The PRHR Hx heat rejection fractions are shown in Figure 5.3 as a function of time for test NRC-5002. It is interesting to note that approximately 60% of the heat is rejected in Zone 1. Another 20% of the total heat is rejected in Zone 2. The remainder of

the total heat is rejected in Zone 3. The lower horizontal tube section at the outlet of the heat exchanger, Zone 4, does not contribute significantly to the heat removal process for this transient. It is interesting to note that Zone 3 switches importance with Zone two after 12,000 seconds into the test.
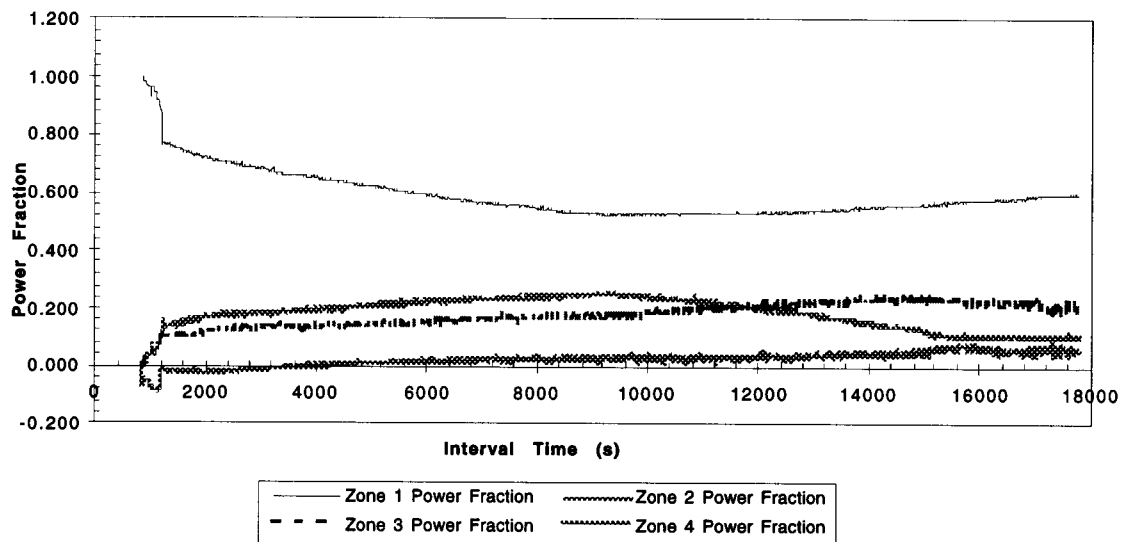
Figure 5.3 APEX PRHR Hx Zonal Power Fractions (NRC-5002)

The PRHR Hx heat rejection fractions for test NRC-5102 are shown in Figure 5.4 as a function of time. Approximately 60% of the heat is rejected in Zone 1 as in NRC-5002. Another 20% of the total heat is rejected in Zone 2 and the remainder of the total heat is rejected in Zone 3. The lower horizontal tube section at the outlet of the heat exchanger, Zone 4, does not contribute significantly to the heat removal process until later in the test when the fluid around the PRHR Hx has reached saturation conditions. As with NRC-5002, Zone 3 switches importance with Zone two after 12,000 seconds into the test. This phenomenon is discussed in the next section.
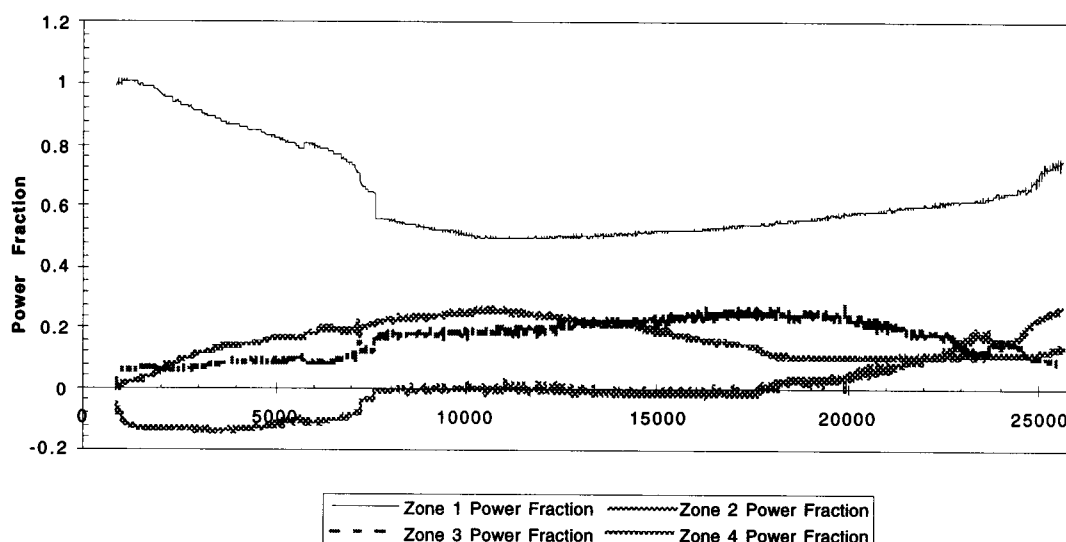
Figure 5.4   APEX PRHR Hx Zonal Power Fractions (NRC-5102)

5.3   Effect of IRWST Thermal Stratification on PRHR Hx Heat Rejection

The axial temperature profile in the IRWST was recorded during both tests by a thermocouple rake inside the IRWST as shown in Figure 2.5.   The IRWST fluid temperature measurements demonstrate that thermally stratified conditions developed during the test. At the beginning of the test, the IRWST was at a uniform temperature. As the test progressed, the upper portion of the IRWST was heated more than the lower portion.   The non-uniform heating of the IRWST is attributed to the system geometry. That is, the hot primary system fluid enters at the upper horizontal section of the PRHR Hx which resides in the upper portion of the IRWST.   The majority of the heat transfer takes place at this elevation.

The heat rejection of each zone of the PRHR Hx was affected by the IRWST thermal stratification. When the test began, the upper portion of the PRHR Hx rejected a much greater portion of the heat because the saturation layer inside the IRWST had not yet developed in that region. As the saturation layer grew to encompass Zone 1, heat rejection in that zone decreased. However, heat rejection in the remaining zones increased,

compensating for the reduction in Zone 1 heat rejection. The total core heat load continued to be removed.

At approximately 9200 seconds for NRC-5002 or 11,000 seconds for NRC-5102, Zone 1 heat rejection began to slowly increase. This may have been due to the development of a flow pattern within the IRWST that enhanced the convective heat transfer in the upper portion of the IRWST. This is discussed in the next section.

NRC-5102 is an extension of the same test as NRC-5002 so as one might expect the heat rejection in each zone shows similar results to NRC-5002.

5.4   Boiling and Flow Patterns Inside the IRWST

Videotape of the PRHR Hx and the upper portion of the IRWST during NRC-5002 revealed that a thermal layer developed at the top of the IRWST. When the IRWST fluid reached saturation conditions at the top of the heat exchanger tubes, boiling on the tube surfaces was significantly enhanced. Later in the transient, bulk motion of the saturation layer could be discerned. It consisted of an azimuthal circulation that did not significantly mix the upper and lower elevations of the IRWST. It is possible that the presence of this circulation pattern caused the increase in Zone 1 heat rejection that was observed 9200 seconds into the test.

Figures 5.5 through 5.7 illustrate the boiling and flow circulation within the IRWST. Figure 5.5 shows the initial conditions in the IRWST prior to the start of boiling. (Note that the distortion of the PRHR inlet tubes is due to light refraction in the water.) Figure 5.6 indicates that the saturation layer has grown to Zone 1. Figure 5.7 shows that the saturation layer has grown to encompass Zone 2. Both Zones show an increase in boiling as they are covered by the saturation layer. The videotape reveals that the saturation layer actually has an azimuthal motion.

Figure 5.5   PRHR Hx at Time t=0 seconds (NRC-5002)
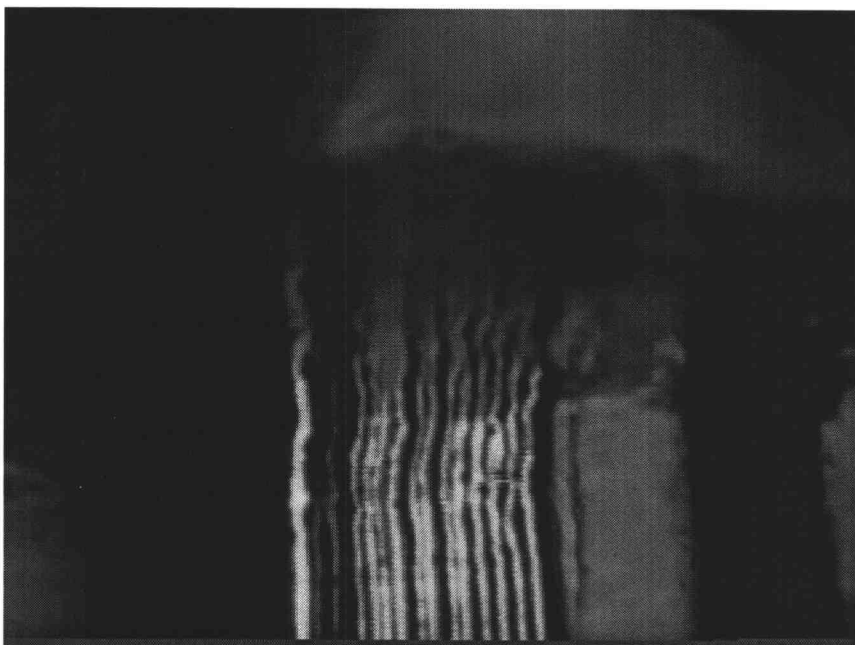
Figure 5.6   PRHR Hx at Time t=9699 seconds (NRC-5002)
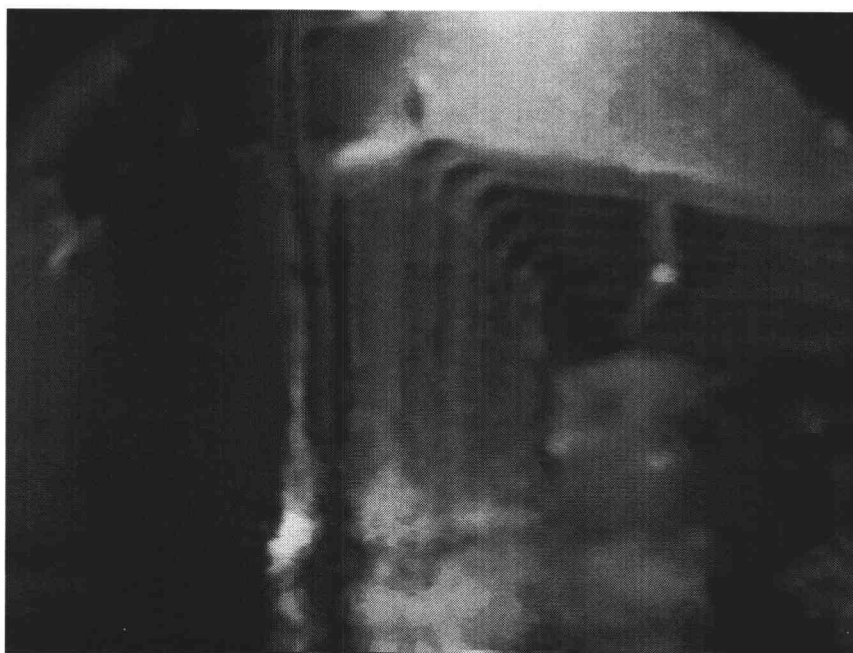
Figure 5.7   PRHR Hx at Time t=10411 seconds (NRC-5002)

Similar phenomena occurred in NRC-5102 but at a slightly different times due do slightly different initial conditions of the plant. The axial temperatures in the IRWST for NRC-5102 are similar to NRC-5002 and are essentially the continuation of the same phenomena, see Figures 5.1 and 5.2. In NRC-5102 all of the fluid surrounding the PRHR Hx reached saturation conditions which is what would have happened if NRC-5002 was run as long. The zones switch over in heat rejection just as in NRC-5002 and as might be expected the thermal layer development in Zone 3 biases the heat rejection to Zone 4 at the end of the test. Zones 4's dominance over Zones 2 and 3 is a logical extension of the phenomena observed in NRC-5002.

5.5   Conclusions of PRHR Hx Characterization During Simulated Station Blackout

OSU APEX tests NRC-5002 and NRC-5102 provided valuable insights into the operation of the PRHR system during a simulated station blackout. The following are the primary conclusions of this study:

- The PRHR Hx is capable of removing core decay heat power for a prolonged period, in a stable manner, without the use of active, forced-flow systems.

- The majority of the core heat is rejected from the top horizontal portion of the PRHR Hx. Approximately 80 percent of the core heat transferred to the IRWST from the top half of the PRHR Hx.

- Thermal stratification in the IRWST affects the PRHR Hx heat rejection process. In particular, as the saturation layer grows to encompass a greater portion of the PRHR Hx, the affected zone becomes less able to reject heat. However, heat rejection in the lower portions of the PRHR Hx continues to increase to compensate for this effect.

- A multidimensional flow pattern develops within the IRWST causing bulk, azimuthal , movement of the saturation layer in the IRWST. This motion does not significantly mix the upper and lower elevations of the IRWST liquid. It may enhance convective heat in the upper portion of the PRHR Hx.

6.　　Conclusions and Recommendations for Further Research

The main conclusions of the PRHR Hx analyses were:

- A bench flow test of the PRHR Hx that obtained a set of pressure drop measurements across the heat exchanger at various fluid flow rates was performed.

- A model of the hydraulic resistance of the heat exchanger using the bench test data was developed.

- A PRHR thermal hydraulic database from APEX Integral System test data was created.

- The heat rejection capability of the PRHR Hx in various operating conditions, including natural circulation and forced flow was studied.

- Heat rejection ability was assessed relative to IRWST fluid temperature stratification.

- The effects of boiling on PRHR Hx heat rejection and other phenomena that develop in the IRWST were studied.

The testing of the PRHR Hx is almost complete. A model of the PRHR Hx hydraulic resistance has been developed, the heat transfer has been studied, and the external phenomena have been observed. To model the PRHR Hx heat rejection under transient conditions the following future research should be performed in the future:

- Perform a three-dimensional (3D) flow analysis for the IRWST.

- Develop predictive heat transfer models to predict PRHR Hx heat transfer coupled with the 3D IRWST flow model.

The remaining portions of study are much more complex than the initial studies and a three dimensional approach will be needed. It should be possible to develop a three dimensional computational fluid dynamic model of the PRHR Hx as built. There are several commercial codes that could be applied to this problem. The studies performed give valuable insight to the PRHR Hx operating phenomena and indicate that the PRHR Hx can be effective in removing decay heat from nuclear cores.

BIBLIOGRAPHY

1.   Reyes, J. N., Jr., L. E. Hochreiter, A. Y. Lafi, and L. K. Lau. *AP600 Low Pressure Integral Systems Test at Oregon State University Facility Scaling Report.* Westinghouse Report WCAP-14270, January, 1995.

2.   ASME NQA-1-1989. *Quality Assurance Program Requirements for Nuclear Facilities.* American Society of Mechanical Engineers, United Engineering Center, 345 East 47th Street, New York, NY 10017.

3.   Quality Assurance Criteria for Nuclear Power Plants and Fuel Reprocessing Plants. *Appendix B of Title 10, Par 50 of the United States Code of Federal Regulations.* US Government Printing Office, issued annually.

4.   LTCT-GAH-001 Revision 2. *AP600 Long Term Cooling Test Project Quality Plan.* Westinghouse Electric Corporation, ESBU Quality Assurance, March 1, 1995.

5.   Welty, J. R., C. E. Wicks and R.E. Wilson. *Fundamentals of Momentum, Heat and Mass Transfer.* John Wiley & Sons Publishing, New York, 1984.

6.   Welty, J. R., C. E. Wicks and R.E. Wilson. *Fundamentals of Momentum, Heat and Mass Transfer.* John Wiley & Sons Publishing, New York, 1984.

7.   Ramsey, F., D. Schafer. *The Statistical Sleuth.* Department of Statistics, Oregon State University, Corvallis, Oregon, 1992.

8.   Stevens, O. L. Software Users Manual. *PRHRVEL- "Passive Residual Heat Exchanger Tube Velocity".* Department of Nuclear Engineering, Oregon State University, Corvallis, Oregon, 1994.

9.   Welty, J. R., C. E. Wicks and R.E. Wilson. *Fundamentals of Momentum, Heat and Mass Transfer.* John Wiley & Sons Publishing, New York, 1984.

10.   Welty, J. R., C. E. Wicks and R.E. Wilson. *Fundamentals of Momentum, Heat and Mass Transfer*. John Wiley & Sons Publishing, New York, 1984.

11.   Moran, M. J., and H. N. Wicks. *Fundamentals of Engineering Thermodynamics*. John Wiley & Sons Publishing, New York, 1988.

12.   White, F. M. *Heat and Mass Transfer*. Addison-Wesley, New York, 1988.

13.   Fraas, A. D. *Heat Exchanger Design*. John Wiley & Sons Publishing, New York, 1989.

14.   Fraas, A. D. *Heat Exchanger Design*. John Wiley & Sons Publishing, New York, 1989.

15.   Reyes, J. N., Jr., L. E. Hochreiter, A. Y. Lafi, and L. K. Lau. *Hot Functional Testing*. Department of Nuclear Engineering, Oregon State University, Corvallis, Oregon. July, 1995.

16.   Reyes, J. N., A. Y. Lafi, S. C. Franz and J. T. Groome. Quick Look Report for OSU APEX NRC-5001. *1-Inch Cold Leg Break with Failure of ADS Valves 1-3*. Department of Nuclear Engineering, Oregon State University, Corvallis, Oregon. July, 1995.

17.   Reyes, J. N., A. Y. Lafi, O. L. Stevens and J. T. Groome. Quick Look Report for OSU APEX NRC-5105. *1/2-Inch Break on Cold Leg #3 with Modified ADS 1,2 and 3 Logic and No CMT Refill*. Department of Nuclear Engineering, Oregon State University, Corvallis, Oregon. March, 1996.

18.   Groome, J. T., J. N. Reyes, J. N., A. Y. Lafi, O. L. Stevens and J. T. Groome. Preliminary Test Analysis Report for OSU APEX NRC-5002. *Station Blackout with Modified ADS Logic, NRC-2, Revision 0*. APEX Long-Term Cooling Test Facility, Department of Nuclear Engineering, Oregon State University, Corvallis, Oregon. December, 1995.

19.   Groome, J. T., J. N. Reyes, J. N., A. Y. Lafi, O. L. Stevens and J. T. Groome. Preliminary Test Analysis Report for OSU APEX NRC-5102. *Station Blackout with Modified ADS Logic, NRC-2, Revision 1*. APEX

Long-Term Cooling Test Facility, Department of Nuclear Engineering, Oregon State University, Corvallis, Oregon. December, 1995.